PURDUE UNIVERSITY
GRADUATE SCHOOL
Thesis/Dissertation Acceptance

This is to certify that the thesis/dissertation prepared

By Asad Raza

Entitled

TUNABLE HYDROGELS FOR PANCREATIC TISSUE ENGINEERING.

For the degree of   Master of Science in Biomedical Engineering

Is approved by the final examining committee:

Chien-Chi Lin

_____Chair_____

Dong Xie

Raghu Mirmira

To the best of my knowledge and as understood by the student in the *Research Integrity and Copyright Disclaimer (Graduate School Form 20)*, this thesis/dissertation adheres to the provisions of Purdue University's "Policy on Integrity in Research" and the use of copyrighted material.

Approved by Major Professor(s): Chien-Chi Lin
_____

Approved by: Edward Berbari   04/05/2013
            Head of the Graduate Program   Date

TUNABLE HYDROGELS FOR PANCREATIC TISSUE ENGINEERING

A Thesis

Submitted to the Faculty

of

Purdue University

by

Asad Raza

In Partial Fulfillment of the

Requirements for the Degree

of

Master of Science in Biomedical Engineering

May 2013

Purdue University

Indianapolis, Indiana

ACKNOWLEDGEMENTS

I would like to thank my thesis advisor, Dr. Chien-Chi Lin for his time, valuable guidance, and support throughout the course of my master's and thesis project. Dr. Lin was really kind, and shared his research and graduate experiences with me, which allowed me to successfully complete my thesis project.

I would like also like to thank my advisory committee members, Dr. Dong Xie and Dr. Raghu Mirmira for their provisions, help and feedback throughout this thesis project. I would like to extend my appreciations to the members of Lin Research Group: Dr. Chang Seok Ki, Han Shih, Yitting Hao, Arika Kemp, Andrew Freaser and Jenny Lin for all their assistance and accommodations.

I would like to thank Dr. Hiroki Yokota, Nancy Tanjung, Andy Chen, Dr. Mirmira's Lab, Andrew Templin, Corey Lin, Vincent Herring and Karl Dria for all their technical assistance. I would also like to thank Ms. Valerie Lim, Subramanian Dharmarajan and Akshayalakshmi Sridhar for assisting me in formatting this thesis.

I extend my special thanks to Department of Biomedical Engineering, specially, Dr. Edward Berbari, Pr. William Combs and Shelly Albertson for their outstanding support, kindness and generosity.

Lastly, I would to thank and convey my love to my family: Dr. Muhammad Raza (Dad), Mrs. Rukhsana Raza (Mom), Ahmed Raza, Faryal Raza and Mishal Raza for their love, prayers and support throughout this journey.

TABLE OF CONTENTS

LIST OF FIGURES

ABSTRACT

Raza, Asad. M.S.B.M.E, Purdue University, May 2013. Tunable Hydrogels for Pancreatic Tissue Engineering. Major Professor: Chien-Chi Lin.

Type I diabetes is an autoimmune disorder characterized by the loss of insulin producing islet cell mass. While daily insulin injection provides an easy means of glycemic control, it does not prevent long-term complications associated with diabetes. Islet transplantation has been suggested as a permanent cure for type 1 diabetes. However, the recurrence of host immunity and shortage of donor islets hinder the prevalence of islet transplantation. Biomaterial strategies provide an alternative route to solving the problems associated with host immune response and shortage of donor islets. One highly recognized platform for achieving these goals are hydrogels, which are hydrophilic crosslinked polymers with tissue-like elasticity and high permeability. Hydrogels prepared from poly(ethylene glycol) (PEG) derivatives are increasingly used for a variety of tissue engineering applications, including encapsulation of pancreatic islets and serving as a material platform for pseudo-islet differentiation. PEG hydrogels formed by mild and rapid thiol-ene photo-click reactions are particularly useful for studying cell behaviors in three-dimension (3D). Thiol-ene PEG-based hydrogels can be rendered biodegradable if appropriate macromer and cross-linker chemistry is employed. However, the influence of hydrogel matrix properties on the survival, growth, and morphogenesis of cells in 3D has not been fully evaluated. This thesis aims at using norbornene-functionalized PEG macromers to prepare thiol-ene hydrogels with various stiffness and degradability, from which to study the influence of hydrogel properties on pancreatic cell fate processes in 3D. Toward establishing an adaptable hydrogel platform

for pancreatic tissue engineering, this thesis systematically studies the influence of hydrogel properties on encapsulated endocrine cells (e.g., MIN6 β-cells) and exocrine cells (PANC-1 cells), as well as human mesenchymal stem cells (hMSC). It was found that thiol-ene photo-click hydrogels provide a cytocompatible environment for 3D culture of these cells. However, cell viability was negatively affected in hydrogels with higher cross-linking density. In contrast to a monolayer when cultured on a 2D surface, cells with epithelial characteristic formed clusters and cells with mesenchymal features retained single cell morphology in 3D. Although cells survived in all hydrogel formulations studied, the degree of proliferation, and the size and morphology of cell clusters formed in 3D were significantly influenced by hydrogel matrix compositions. For example: encapsulating cells in hydrogels formed by hydrolytically degradable macromer positively influenced cell survival indicated by increased proliferation. In addition, when cells were encapsulated in thiol-ene gels lacking cell-adhesive motifs, hydrolytic gel degradation promoted their survival and proliferation. Further, adjusting peptide crosslinker type and immobilized ECM-mimetic bioactive cues provide control over cell fate by determining whether observed cellular morphogenesis is cell-mediated or matrix-controlled. These fundamental studies have established PEG-peptide hydrogels formed by thiol-ene photo-click reaction as a suitable platform for pancreatic tissue engineering.

1. INTRODUCTION

1.1 Pancreas, Type I Diabetes and Therapeutic Approach

Pancreas is composed of functionally distinct endocrine and exocrine machineries. The exocrine region is formed by acinar and duct cells making up to 95–98% of the pancreas. The function of the exocrine part is to produce digestive enzymes and electrolytes, which help in nutrient digestion and absorption in the gastrointestinal tract [1]. On the other hand, endocrine cells form aggregates scattered throughout the exocrine pancreas in the form of islets of Langerhans [1, 2]. The islets are made up of five principle endocrine cell types categorized by the hormone they secrete, which are: insulin-producing β-cells, glucagon-producing α-cells, somatostatin-producing δ-cells, ghrelin-producing ε-cells and pancreatic polypeptide-producing PP-cells [1]. The main functions of these endocrine hormones are: insulin stimulates glucose uptake, glucagon mobilizes glucose from the liver into the circulation, somatostatin inhibits both α- and β-cell secretions, pancreatic polypeptide exerts an inhibitory role in pancreatic exocrine secretion and ghrelin inhibits insulin secretion [1-4]. In summary, all endocrine cells play an important role in maintaining blood glucose levels.

Insulin secreting β-cells are one of five major types of cells that make up the mammalian pancreatic islet. They make up 1–2% of the total cell mass of the pancreas and 65–85% of the Langerhans islets cells [2-4]. As mentioned earlier, β-cells secrete the hormone insulin in response to nutrients, hormones and neuronal stimuli and hence play a pivoting role in the maintenance of glucose homeostasis. The endocrine function of β-cells can be negatively affected if a person has type I diabetes, type II diabetes or pancreatic cancer.

Insulin dependent (Type 1) diabetes is an autoimmune disease caused by β-cell-targeting auto-immunity [5, 6]. Hyperglycemia arises due to the loss of β-cell mass, hence exogenous insulin treatment is required to restore normal blood glucose homeostasis. The most common glycemic therapy is via daily insulin injections, which not only cause patients discomfort, but also accumulate risks of hypoglycemia and insulin-resistance in the long-term [7]. To alleviate reliance on daily insulin injections, several therapeutic interventions have been adopted, including whole pancreas transplantation [8] and islet transplantation using the Edmonton protocol [9, 10]. The latter involves infusing donor islets in the portal vein, followed by an improved immunosuppressive regimen. Islet transplantation provides better glycemic control over conventional exogenous insulin therapy and is considered a safer alternative to whole pancreas transplantation [11, 12]. Unfortunately, the clinical prevalence of this technique is greatly hindered by the shortage of donor islets for transplantation (islets from at least two donors are needed for one recipient), poor viability of the isolated and transplanted islets *in vivo*, and recurrence of immune rejection [13-16].

Due to the threat posed by type I diabetes, the number of studies analyzing the mechanisms that govern β-cell proliferation and growth in physiological and pathological conditions has increased exponentially during the last few decades [3]. Most in vitro studies use cell lines, such as Murine β-cell line (MIN6) (due to islet-like sensitive nature of these cell) in order to analyze and characterize matrix conditions influencing pancreatic β-cell survival and functioning in 3D culture [17]. In conjunction with pancreatic β-cells, mesenchymal stem cells (MSCs) have been used to improve islet transplantation outcome (most likely due to paracrine effects) [18-21].

Many studies have also focused on differentiating stem or precursor cells into insulin-secreting cells [22-25], while others have focused on developing *in vitro* culture techniques to expand/preserve these cells [8, 26, 27]. One widely researched culture platforms is semi-permeable polymeric capsule. The premise of this technique is that the encapsulated islet cells are protected from direct contact of host immune cells and large

antibodies, while the semi-permeable membrane still allows facile exchange of nutrients and cell metabolic products [15, 28-31]. Various cytocompatible natural and synthetic biomaterials have been developed for cell encapsulation [15, 32-34], but it remains a challenge to create a suitable three-dimensional biomimetic microenvironment for encapsulation of islet cells. This is because pancreatic β-cells are known to undergo apoptosis easily when exposed to environmental stresses such as hypoxic and oxidative conditions [35-37]. As a result, the encapsulation conditions suitable for other cells that are more robust (e.g., fibroblasts, mesenchymal stem cells, etc.) are often sub-optimal for β-cell encapsulation. While efforts have been made towards creating material platform for immunoisolation and material-based differentiation of cells to insulin secreting cells, there exists a critical need to develop a material platform for safe encapsulation and long-term culture of β-cells and islets. Such a material platform may also serve as a foundation for generating large quantity of insulin-secreting cells to overcome the obstacle of donor islet shortage.

1.2   PEG-Based Hydrogels

Hydrogels are hydrophilic crosslinked polymers with exceptional potential as scaffolding materials for repairing and regenerating tissues [38-40]. The high water content of hydrogels permits easy diffusion of oxygen and exchange of nutrients and cellular metabolic products, all of which are crucial to maintaining cell viability. In addition, hydrogels are excellent carriers for controlled release and cell delivery due their high tenability [39]. Many potential hydrogel systems have been explored employing both natural and synthetic polymer, specific examples to which include: Ionically crosslinked alginate–poly(lysine) system, copolymer of poly(acrylonitrile) and poly(vinyl chloride) (PAN–PVC), poly(N-isopropylacrylamideco – acrylic acid) gel, poly(ethylene glycol) (PEG), poly(vinyl alcohol) (PVA) and poly(Nisopropylacrylamide) (PNIPAAM) [17, 41]. Synthetic hydrogels like PEG-based hydrogels have advantages over natural hydrogels, due to their ability for easy photopolymerization, easy control of scaffold

architecture and chemical compositions, adjustable mechanical properties and tunable matrix composition to match the target tissue [41-44].

Synthetic hydrogels such as those prepared from poly(ethylene glycol) (PEG) are increasingly used in tissue engineering applications [38, 39, 45-48], such as immunoisolation [29-31, 49, 50] and controlled cell differentiation [51, 52], largely due to their cytocompatibility, tissue-like elasticity, and high tunability in material physical and mechanical properties [17, 38, 48, 53, 54]. Additionally, PEG hydrogels provide a unique niche for cell encapsulation with high biocompatiblility and high permeability which allows for the diffusion of nutrients and metabolites, while protecting cells against host immune cells [15, 35, 39]. PEG-based hydrogels have been successfully used to encapsulate a variety of cell types, including pancreatic β-cells, stem cells, endothelial cells, epithelial cells, etc. Further, defined instructive cues can be incorporated in PEG-based hydrogels to enhance cell survival and functioning. Moreover, the photopolymerization methods used to prepare PEG-based hydrogels have profound impact on cell viability during *in situ* cell encapsulation, especially for radical sensitive cells [27].

1.3   Chain-Growth Photopolymerization

Although a commonly used hydrogel platform, studies have shown that PEG diacrylate (PEGDA) hydrogels formed by chain-growth photopolymerizations (**Figure 1.1a**) have a tendency to damage encapsulated cells during network crosslinking and *in situ* cell encapsulation [27]. The cellular damage was largely attributed to radical species generated by the photoinitiator molecules, which propagate through the vinyl groups on PEGDA to crosslink polymer chains into hydrogels. Unfortunately, these radical species also cause stresses and cellular damage during cell encapsulation, unless bioactive or cyto-protective motifs are conjugated in the hydrogel network [32, 35, 49, 55, 56]. In order to obtain a higher mesh size for better diffusion and cell survival, higher molecular

weights PEGDA are often used for cell encapsulation. This, however, compromises polymerization kinetics and causes sub-optimal gel biophysical properties [27, 49, 57].

In addition, hydrogels prepared from chain-growth photopolymerization may cause protein de-activation or irreversible conjugation within the cross-linked polymer network [58]. It is believed that high radical concentrations and long half-life of the radical species are responsible for these adverse reactions [59]. Adding to the above mentioned disadvantages, it is very difficult to recover cell structures from PEGDA hydrogels due to the heterogeneity and non-degradable nature of the crosslinked networks. While protease-sensitive peptides can be incorporated into PEG macromer backbone to render the otherwise inert PEGDA hydrogels sensitive to enzymatic cleavage, the conjugation often uses expensive reagents and the resulting networks still contain high degree of heterogeneity due to the nature of chain-growth polymerization [60-62].

(a)
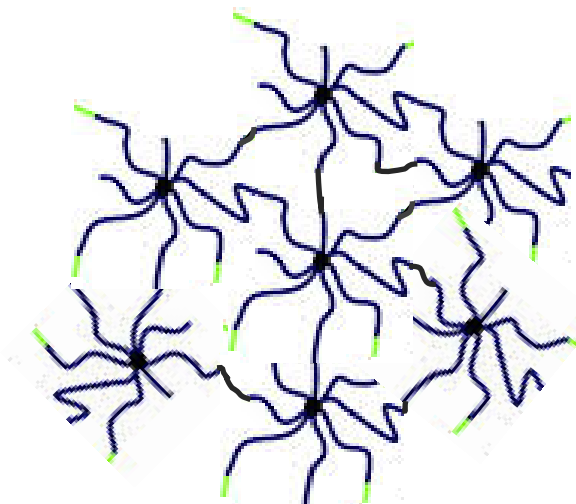
(b)
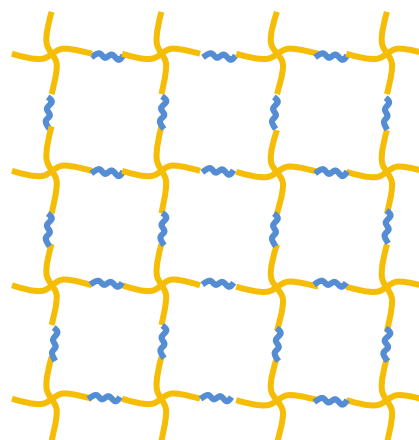
Figure 1.1. Schematic of hydrogel network structure formed by (a) Chain-growth photopolymerization and (b) Step-growth photopolymerization (Schematic not to scale)

1.4   Step-Growth Thiol-Ene Photopolymerization

Initially introduced by Fairbanks and Anseth *et al.* in 2009, PEG-peptide hydrogels fabricated from step-growth thiol-norbornene photo-click reactions (**Figure 1.1b**) have proven to be an attractive class of biomaterials for controlling protein delivery and promoting tissue regeneration [63-66]. Step-growth thiol-ene photopolymerization have been shown to exhibit preferential properties for cell encapsulation over hydrogels formed by chain-growth photopolymerization [27]. The superior gelation kinetics of thiol-ene hydrogels is attributed to the 'click' nature of reaction between thiol and ene functionalities. Compared to chain-growth polymerization of PEGDA, thiol-ene reaction is less oxygen inhibited which results in faster gelation rate [67, 68]. Thiol-ene hydrogels also have higher polymerization efficiency, better gel biophysical properties, highly tunable gelation kinetics, idealized network structures, as well as versatility in bioconjugation compared to chain-growth PEGDA hydrogels [27, 63]. All these factors combined result in limited cellular damage caused by radical species during thiol-ene step-growth photopolymerization [27]. Although thiol-ene hydrogels are increasingly used as synthetic extracellular matrix mimics for 3D cell culture, studies correlating their material properties and superior cytocompatibility remain limited and warrant further investigation.

Due to milder reaction conditions and extremely rapid gelation kinetics compared to other reaction schemes, thiol-ene hydrogels allow for the formation of a superior synthetic microenvironment for cell encapsulation. Using the thiol-norbornene photopolymerization scheme, we have recently shown that radical-sensitive pancreatic β-cells can be safely encapsulated with no significant cellular damage [27]. MIN6 β-cells were able to proliferate in thiol-norbornene hydrogels even at a very low cell packing density (2×10^6 cells/mL) and without the presence of extracellular matrix (ECM) molecules. In contrast, MIN6 cells encapsulated in chain-growth PEGDA hydrogels did not survive at this low cell packing density [27, 55]. When appropriate peptide substrates (e.g., CGGY↓C, where arrow indicates chymotrypsin cleavage site) were used as thiol-

norbornene hydrogel cross-linker, cell spheroids generated *in situ* can be rapidly recovered via enzyme-mediated gel erosion [27, 69].

In a separate study using experimental investigation and mathematical modeling, *Shih & Lin* reported that thiol-ene gels formed by multi-arm PEG-ester-norbornene and dithiol-containing linker (e.g., dithiothreitol (DTT) or bis-cysteine-bearing peptides) were susceptible to base-catalyzed hydrolytic degradation [70]. Depending on the gel formulations, the hydrolytic degradation rate of these thiol-ene hydrogels could be tuned from weeks to months. Although these studies have elucidated the biophysical aspects of thiol-norbornene hydrogels, a potential link between these properties and the fate of encapsulated cells has not been established.

1.5   Pancreatic Exocrine Adenocarcinoma Cells for Endocrine Differentiation

Initially introduced as continuous tumor – cell line in 1975 by Lieber *et al*., PANC-1 cells are human pancreatic adenocarcinoma cells, clonally derived from the epithelium of the pancreatic duct carcinoma [71]. Immediately after establishment, research focus was to study the properties of PANC-1 cells in comparison to other existing epithelial cell lines [72]. It was found that when grown on plastic substrate, PANC-1 cells form squamous type of epithelium [72, 73]. Now also known as pancreatic ductal epithelial cells, PANC-1 cells have been utilized on multiple occasions to study pancreatic carcinoma both *in vivo* and *in vitro* [74-78]. Further, these cells have also been used to understand cancer metastasis at both protein and genetic levels. For example, Binker *et al.* utilized PANC-1 cells to investigate the role of MMP-2 in pancreatic cancer cell mediated tissue invasion [79]. In a more recent study, Zhu *et al*. exploited PANC-1 cell features to study the effect of integrin-linked kinase (ILK) gene silencing on cancer cell proliferation, migration and invasion [80]. In addition to cancer metastasis, recently this epithelioid cell line has been utilized for studying exocrine to endocrine differentiation [81-84]. Studies have shown that PANC-1 cells when given appropriate

soluble cues can be differentiated into insulin secreting cell clusters that these differentiated cells may serve as an alternative cell source to treat type I diabetes [82].

In spite of the diverse applications of PANC-1 cells not limited to cancer metastasis and endocrine differentiation, most of the studies performed have only evaluated cell features in two – dimensional (2D) culture. While these studies have revealed important information about epithelial cell behavior, the application remains limited due to discrepancy between *in vitro* and *in vivo* cell behavior. Recent efforts have recognized the importance of three – dimensional (3D) models towards biomedical applications for both fundamental and applied cancer studies, but there has only been modest progress towards this goal. For example, studies performed using NanoCulture plates, Matrigel and collagen gels (all with limited matrix tunabilityin gel biophysical properties) as platforms for PANC-1 and other epithelial cell culture have revealed information about role of matrix metalloproteinase (MMP) [85], transforming growth factor (TGF-β) [86, 87], and epidermal growth factor receptor (EGFR) [79] on cell spreading, metastasis and tumor growth. Despite of the limited success in studying PANC-1 metastasis in 3D, no prior attempt has been made to establish a well-defined and highly tunable matrix for studying and controlling morphogenesis of PANC-1 cells in 3D.

2. OBJECTIVES

The main objective of this thesis was to systematically study the parameters affecting pancreatic endocrine and exocrine cell fate in 3D. The overarching goal of this project was to develop a highly adaptable hydrogel platform for pancreatic tissue engineering applications, including forming immunoisolation barriers for endocrine islets and generating insulin-secreting cells from epithelial tissues. Specifically, this thesis studied the effect of hydrogel matrix properties, including cross-linking density and degradation rate, on the survival and proliferation of MIN6 beta cells and pancreatic ductal epithelial cells (PANC-1) was studied. Specific objectives are:

2.1 Characterize Hydrogel Matrix Properties

Thorough understanding of hydrogel matrix properties is the prerequisite to study cell behaviors in 3D. Utilizing hydrogels formed by thiol-ene step-growth photopolymerization, the first objective of this thesis was to characterize hydrogel swelling and stiffness, two critical parameters affecting cell survival in 3D. The results from these fundamental studies will establish a hydrogel platform with improved cytocompatibility and tunability for pancreatic tissue engineering.

2.2 Investigate the Survival and Proliferation of Pancreatic Beta Cells and Human Mesenchymal Stem Cell in 3D

After obtaining basic understanding of hydrogel matrix properties, the second objective of this thesis was to evaluate the survival and morphology of MIN6 β-cells or hMSCs encapsulated in thiol-ene hydrogels with highly defined and tunable properties.

The goal of these studies is to establish a hydrogel platform with improved matrix properties for supporting the survival and function of pancreatic beta cells.

2.3   Establish Tunable Hydrogel Niches for Culturing Pancreatic Exocrine Cells

Alternative insulin-secreting cell sources are urgently needed for islet transplantation. The third objective of this thesis was to study the growth and morphogenesis of pancreatic adenocarcinoma cell (PANC-1 cell) in 3D. The understanding of PANC-1 cell behaviors will establish foundation for future endocrine differentiation of these cells in 3D.

3.   MATERIALS AND METHODS

3.1   PEG4eNB, PEG4aNB, and Photoinitiator LAP Synthesis

Degradable PEG-tetra-ester-norbornene (PEG4eNB, **Figure 3.1a**) was synthesized according to an established protocol with slight modifications [63]. Briefly, 4-arm PEG-OH (Jenkem Technology USA) was dried in a vacuum oven overnight and dissolved in anhydrous toluene. Toluene was evaporated using a rotary evaporator and the dried 4-arm PEG was dissolved in anhydrous dichloromethane (DCM). In a separate flask, 5-norbornene-2-carboxylic acid (5 eq.) was reacted with N,N'-dicyclohexlycarbodiimide (DCC, 2.5 eq.) in anhydrous DCM for at least 15 minutes at room temperature to form norbornene anhydride. The later was filtered through a fritted funnel and added drop-wise into a second flask (placed in an ice bath) containing dried 4-arm PEG-OH, 4-(dimethylamino)pyridine (DMAP, 0.5 eq.), and pyridine (5 eq.) in DCM. All reactions were performed under nitrogen. After overnight reaction, the product (PEG4eNB) was filtered, washed with 5 wt.% sodium bicarbonate to remove unreacted norbornene acid and dried over sodium sulphate. The product was then filtered and precipitated in cold ethyl ether. The filtered product was re-dissolved in DCM and re-precipitated in cold ethyl ether to obtain the final product. PEG4eNB was dried overnight in vacuo and the degree of functionalization (> 85 %) was measured using proton NMR (Brucker 500). Note: All chemicals were procured from Sigma-Aldrich unless noted otherwise.

Non-degradable PEG-tetra-amide-norbornene (PEG4aNB, **Figure 3.1b**) was synthesized by reacting 4-arm PEG-NH$_2$ (Jenkem Technology USA) with norbornene carboxylic acid using HBTU (2-(1H-Benzotriazole-1-yl)-1,1,3,3-tetramethylaminium hexafluorophosphate) /HOBT (1-Hydroxybenzotriazole anhydrous) coupling chemistry.

Briefly, 4-arm PEG-NH2 was dried in a vacuum oven overnight and dissolved in anhydrous dimethylformamide (DMF). In a separate flask, norbornene carboxylic acid (5 eq.) was activated by HBTU and HOBT (5.5 eq.) in DMF for 3 minutes at room temperature. To the activated acid solution, DIEA (6 eq.) was added and further reacted for 5 minutes under nitrogen. The mixture was then added drop wise to the flask containing 4-arm PEG-NH$_2$ and allowed to react overnight. PEG4aNB was obtained by precipitation in cold ether and further purified using protocol similar to PEG4eNB purification procedure. The degree of functionalization ($>$ 85 %) was measured using proton NMR.

The photoinitiator lithium arylphosphinate (LAP) was synthesized according to a published protocol without modification [88].

(a)

4-arm PEG-OH → DCC / DMAP / Pyridine / DCM → **PEG4eNB**

(b)

4-arm PEG-NH$_2$ → HBTU / HOBT / DMF → **PEG4aNB**
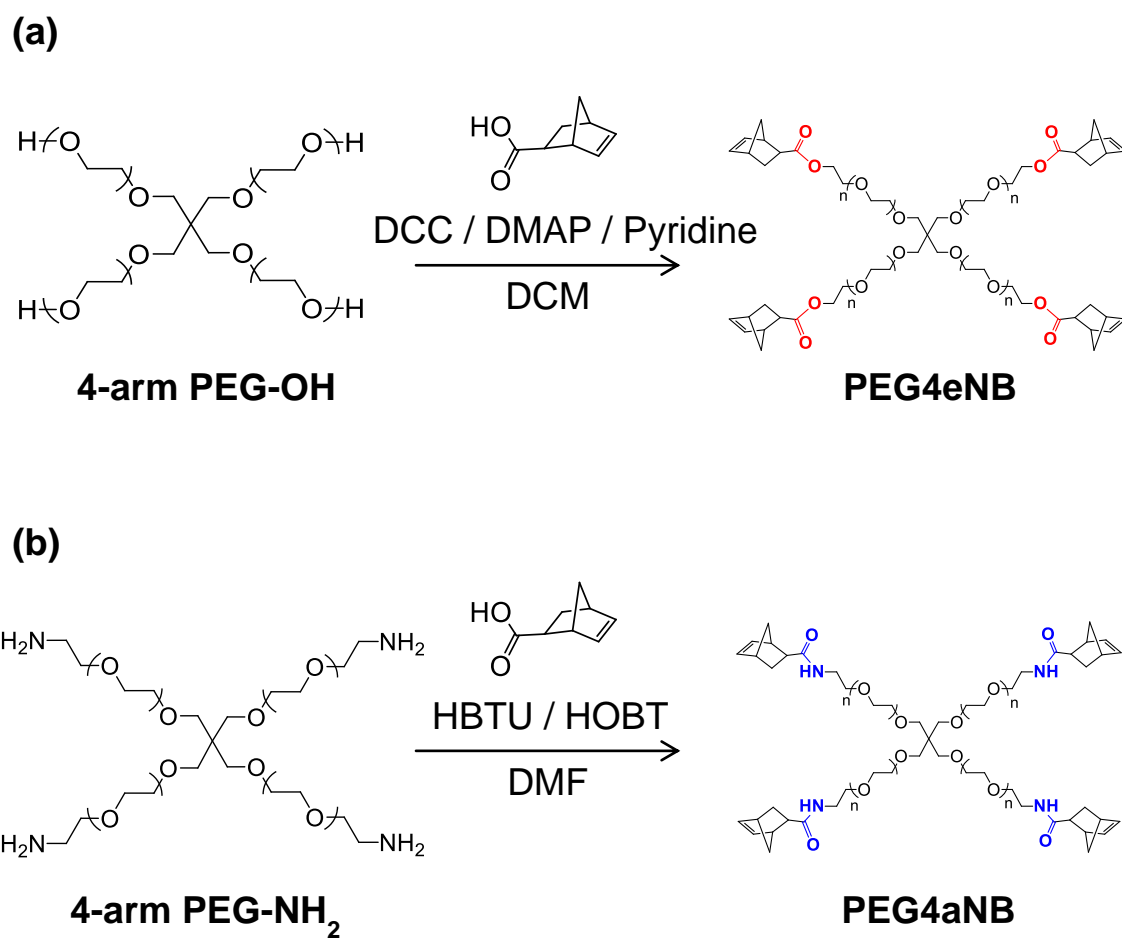
Figure 3.1. Reaction schematic of (a) ester linkage containing hydrolytically degradable PEG-tetra-norbornene (PEG4eNB) and (b) amide linkage containing non-degradable PEG-tetra-norbornene (PEG4aNB) synthesis

3.2   Peptide Synthesis

Fmoc-amino acids, Fmoc-Rink-amide MBHA resin, and peptide synthesis reagents were purchased from Anaspec Inc or Chempep Inc. All peptides (CGGYC, KCGPQGPAGQCK, KCGPQGIWGQCK, CGRGDS and KCYIGSR (**Table 3.1**)) were synthesized using standard solid phase peptide synthesis (SPPS) chemistry in a microwave peptide synthesizer (CEM Discover SPS) following the manufacturer's recommended synthesis procedures.   Terminal cysteines were added for thiol-ene reaction. The peptides were also cleaved in the microwave peptide synthesizer (38 °C, 20 W, 30 min) using a cleavage cocktail containing 95 % trifluoroacetic acid (TFA), 2.5 % water, and 2.5 % triisopropylsilane (TIS) in the presence of 5 wt/v.% phenol. Crude peptides were precipitated in cold ethyl ether, dried overnight in a desiccator and purified using preparative scale HPLC (PerkinElmer Flexar System). All peptides were purified to atleast 90% purity and characterized by analytical scale HPLC and mass spectrometry (Agilent Technologies). HPLC grade acetonitrile and water were acquired from Fisher Scientific and VWR International, respectively. Purified peptides were lyophilized and stored in -20 ^{o}C.   The concentration of thiol groups on purified cysteine-containing peptides was quantified using Ellman's reagent (PIERCE) [69].

Table 3.1. Cross-linkers used to form thiol-ene hydrogels.

Label	Linker chemistry	Linker degradability	Gel degradability
DTT	Dithiothreitol	Non-cleavable	Slow hydrolytic
CGGYC	CGGY[a]C	Chymotrypsin sensitive	Fast hydrolytic & enzymatic
MMP$_{scrm}$	KCGPQGPAGQCK	Non-cleavable	Fast hydrolytic
MMP$_{Linker}$	KCGPQG[b]IW[a]GQCK	MMPs & chymotrypsin sensitive	Fast hydrolytic & enzymatic

[a] P1 positions for chymotrypsin-mediated cleavage
[b] P1 position for metalloproteinases (MMPs)-mediated cleavage

3.3   Hydrogel Fabrication and Characterization

Thiol-norbornene hydrogels formed by step-growth photopolymerization were fabricated using PEG4eNB or PEG4aNB (20 kDa) and di-thiol crosslinkers, such as DTT (D) or bis-cysteine containing peptide CGGYC (C) [27] or KCGPQGPAGQCK (MMP$_{scrm}$ / M$_s$) [89] or KCGPQGIWGQCK (MMP$_{Linker}$ / M$_L$) [90, 91] (**Table 1**). Radical-mediated thiol-norbornene photopolymerization was initiated using 1 mM LAP dissolved in PBS under long-wave UV light exposure (365 nm, 5 mW/cm^2) for 3 minutes (**Figure 3.2**). For all hydrogel formulations, a stoichiometric ratio between thiol and norbornene groups was maintained. Gels (50 μL) were formed in 1 mL disposable syringes with cut-open tips.

Following thiol-norbornene photopolymerization, hydrogels were incubated at 37 ^{o}C in ddH$_2$O on an orbital shaker for 24 hours to remove all unreacted macromers. The gels were then dried in vacuum for 24 hours to obtain dried gel weight (W_{dry}). Dried gels

were then incubated in PBS at 37 $^{\circ}$C on an orbital shaker. At predetermined time points (i.e. 2, 4, 7, and 10 days), hydrogel swollen weights ($W_{swollen}$) were measured gravimetrically and were used to calculate the mass swelling ratio (q), which is defined as: $W_{swollen}/W_{dry}$. The mass swelling ratios were used to calculate hydrogel mesh size based on the Flory-Rehner theory as described elsewhere [40].
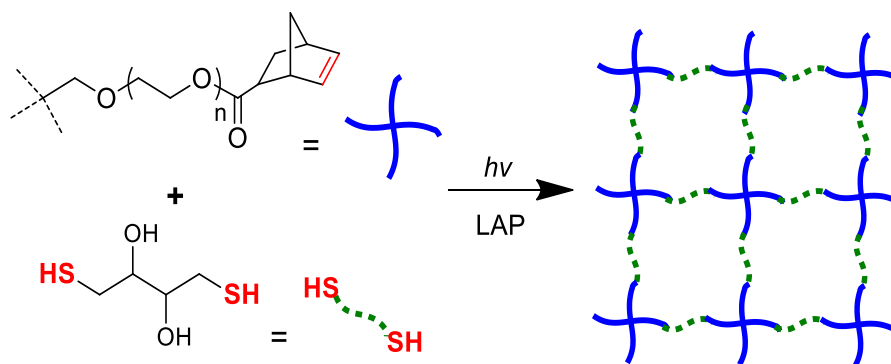
Figure 3.2. Schematic of thiol-ene photo-click reaction to form PEG-based hydrogels. Gels are formed under UV light (365nm, 5mW/cm^2) exposure with 1 mM of lithium arylphosphanate (LAP) as photoinitiator. Only one arm is shown in the structure of PEG-tetra-norbornene (PEG4NB). Any multi-functional linker containing more than two thiol moieties, such as dithiothreitol (DTT) shown in the schematic, can be used as gel cross-linker.

3.4   Oscillatory Rheometry

Rheometrical shear modulus measurements were performed according to published protocol [70]. Briefly, thiol-norbornene hydrogel slabs were prepared between two glass slides and circular discs punched out from the hydrogel slabs. Rheological oscillatory measurement to measure shear modulus immediately following photopolymerization was performed on Bohlin CVO 100 digital rheometer. Data was analyzed and recorded as mean $\pm$ SD for 4 independent samples per test group.

3.5   Cell Culture

Murine pancreatic β-cells (MIN6) (courtesy of Anseth Research Group) were maintained in high glucose DMEM (HyClone) containing 10 % fetal bovine serum (Gibco), 1X Antibiotic-Antimycotic (Invitrogen, 100 U/mL penicillin, 100 μg/mL streptomycin and 250 ng/mL Fungizone), and 50 μM β-mercaptoethanol. Human mesenchymal stem cells (hMSCs) were isolated from human bone marrow (obtained from Lonza) and maintained in low glucose DMEM (HyClone) containing 10 % fetal bovine serum (Gibco), 1X Antibiotic-Antimycotic (Invitrogen, 100 U/mL penicillin, 100 μg/mL streptomycin and 250 ng/mL Fungizone), and 1 ng/mL recombinant human bFGF (PeproTech). PANC-1 cells (obtained from ATCC) were maintained in high glucose DMEM (HyClone) containing 10 % fetal bovine serum (Gibco) and 1X Antibiotic-Antimycotic (Invitrogen, 100 U/mL penicillin, 100 μg/mL streptomycin and 250 ng/mL Fungizone). Cells were cultured in tissue culture plastic kept at 37 $^{\circ}$C and 5 % CO_2 and the culture mediums were changed every 2 to 3 days. [hMSCs were used in passages 2-4.]

3.6   Cell Encapsulation

Cell encapsulation was performed using a procedure similar to the gel fabrication method described earlier. Briefly, MIN6 β-cells or hMSCs or PANC-1 cells (at a cell packing density of 2×10^6 cells/mL [27] or 5×10^6 cells/mL [92] or 2×10^6 cells/mL (determined experimentally), respectively) were suspended in pre-polymer solutions containing PEG macromer, cross-linker, CRGDS or KCYIGSR (for some experimental groups) and photoinitiator, and exposed to UV light (365 nm, 5mW/cm^2) for 2 minutes. Cell-laden hydrogels (25 µL) were maintained in identical cell culture conditions as described earlier on an orbital shaker [69].

3.7   Encapsulated Cell Viability Assays

To measure initial cell viability in hydrogels, cell-laden hydrogels were incubated in buffers containing 75 µL of HBSS (for MIN6 β-cells) or PBS (for hMSCs and PANC-1 cells) and 75 µL of CellTiter Glo® reagent (acquired from Promega) following photopolymerization. After 1 hour of incubation, intracellular ATP concentration was quantified by measuring sample luminescence using a microplate reader (Synergy HT, BioTek Instruments). Intracellular ATP concentrations were interpolated from a series of known ATP monohydrate concentrations.

Qualitative cell viability following photoencapsulation was determined using Live/Dead staining (obtained from Invitrogen) and confocal imaging. Cell-laden hydrogels were incubated in Live/Dead staining solution for 1 hour at room temperature with gentle shaking. Confocal images of the stained samples were obtained using Olympus Fluoview FV100 Laser Scanning Biological Microscope (IUPUI Nanoscale Imaging Center). Z-stack images (100 µm thick, 10 µm per slice) from three samples and at least four random fields were acquired for every experimental condition. A total of at least 12 z-stack images were utilized for counting live (staining green) and dead (staining red) cells for all experimental groups. Cell viability was quantified by calculating percentage of live cells relative to total number of cells.

To monitor long term cell viability and proliferation, cell-laden hydrogels were incubated in 500 μL of 10% AlamarBlue® reagent (acquired from AbD Serotec) in cell culture medium for 16 hours (for MIN6 β-cells) or 14 hours (for hMSCs) or 4 hours (for PANC-1). Following incubation, 200 μL of the media was transferred to a 96-well plate and fluorescence generated due to non-specific cellular metabolic activity was measured using a microplate reader (excitation: 560 nm, emission: 590 nm).

3.8   Morphology Assessment

Z-stack confocal images of Live/Dead staining were also used to visualize cell morphology within hydrogels at day 10 (for every experimental condition). Images from four samples and at least three random fields per sample were acquired for further analysis. All Live/Dead images were analyzed using Olympus Fluoview and NIH ImageJ software. For hMSCs, cell length was defined as the longest end to end distance of a straight line connecting the two end points on a cell. For both MIN6 β-cells and PANC-1 cells, spheroid and cluster sizes were acquired by measuring the spheroid or cluster diameter in both x and y direction and the average of the two diameters was reported as cell spheroid diameter (MIN6 β-cells) or cluster size (PANC-1 cells).

Live/Dead from four samples and at least three random fields per sample were also semi-quantitatively analyzed for PANC-1 cell morphology using Olympus Fluoview. PANC-1 cell morphology was categorized according the following: (I) Single cell; (II) Small rounded and compact clusters; (III) Large and irregular cell clusters; (IV) Small clusters with short cellular protrusions; and (V) Cyst-like cell clusters. Total populations of each category were manually counted.

3.9   Protein Extraction and Western Blot Analysis

Total proteins from encapsulated cells were extracted by first homogenizing cell-laden hydrogels using a VWR^{TM} Pellet Mixer. Homogenized samples were lysed with cell lysis buffer containing: 10 µL of Halt Protease inhibitor, 10 µL of EDTA and 1mM of Phenylmethylsulfonyl Fluoride (PMSF) dissolved in 1 mL of RIPA Buffer. Total extract was cleared by centrifugation at 8000 ẋg for 10 minutes at 4 ^{o}C. Protein extracts were further concentrated in Centrifugal Filter Units (Millipore) at 14000 ẋg for 20 minutes at 4 ^{o}C. Extracted protein concentration was determined by BCA protein quantification assay using Pierce BCA Protein Assay Kit (Thermo Scientific) following manufacturer protocol.

Concentrated protein extracts were then subjected to western blot analysis. Briefly, equal amounts of proteins between groups were loaded on to a 10% Min-PROTEAN TGX Precast Gels (Bio-rad) and subjected to sodium dodecyl sulfate polyacrylamide gels electrophoresis (SDS-PAGE). After complete separation, proteins were transferred on to 0.45µm Immobilon-P PVDF transfer membrane (Millipore) using Trans-Blot Turbo Transfer System's standard semi-dry transfer protocol. The blots were blocked overnight with 5% nonfat milk in TBST solution (1X PBS containing 0.5% Tween-20) at 4 ^{o}C. The blots were then sequentially reacted with diluted primary antibody and HRP conjugated secondary antibody for 1 hour at room temperature. Primary antibodies used: Mouse anti-β-actin (Sigma, 1:1000); Rabbit anti-Vimentin (Cell Signaling, 1:1000); Rabbit anti-Snail (Cell Signaling, 1:500); Rabbit anti-β-catenin (Cell Signaling, 1:1000); Rabbit anti-E-cadherin (Cell Signaling, 1:1000). Secondary antibodies used: HRP-labeled goat anti-rabbit or goat anti-mouse IgG (Cell Signaling, 1:500 to 1:1000). The blots were washed with TBST solution for 1 hour and prepared for chemiluminescence detection using SuperSignal West Pico Detection Kit (Thermo Scientific) according to manufacturer's protocol and imaged using Fuji LAS 3000 imaging system. Band analysis was performed using ImageJ and reported band intensities were relative to β-actin band intensity.

3.10 Whole Mount Immunostaining

Insulin, CD105, F-actin and β-catenin expressions in cells after 10 days of culture in 3D thiol-ene hydrogels were visualized by immunostainig. Cell-laden hydrogels were fixed in 4 % paraformaldehyde at room temperature for 45 minutes with gentle shaking. Samples were then rinsed with PBS and encapsulated cells were permeabilized using 0.5 % Triton X-100 in PBS at room temperature for 45 minutes with gentle shaking. Following permeabilization, samples were washed with PBS and blocked (5% BSA, 5% polyvinylpyrrolidone, and 10% fetal bovine serum) overnight at 4 $^{\circ}$C. Samples were sequentially incubated overnight at 4 $^{\circ}$C in primary antibody (Santa Cruz, 1:100) and fluorophore-conjugated secondary antibody (Cell Signaling and Cytoskeleton, 1:100) solution for Insulin, CD105, F-actin and β-catenin. The samples were rinsed with PBS, further stained with DAPI for 1 hour and washed with PBS. The fluorescence from encapsulated cells was visualized and imaged using confocal microscope.

3.11 Statistical Analysis

All experiments were conducted independently for three times and the results were presented as mean ± SD. Statistical analysis was performed using Excel and GraphPad Prism software. Shear modulus and Intracellular ATP results were analyzed for statistical significance between selected groups using Students' t-test. Cell-viability, spheroid diameter, cluster size and cell morphology data were analyzed using one-way ANOVA followed by a Dunnett post-hoc test. Cell viability and western blotting band intensity data were analyzed using two-way ANOVA followed by Bonferroni's post-hoc test. Difference between conditions was considered statistically significant when $p < 0.05$.

4.   RESULTS AND DISCUSSION

4.1   Characterizing Thiol-Ene Hydrogel Matrix Properties

Hydrogels formed by photopolymerized step-growth thiol-norbornene chemistry (**Figure 3.2**) have proven to be an extremely cytocompatible platform for encapsulation of many cell types including very sensitive cells [27]. Depending on the macromer and cross-linker chemistry, thiol-ene hydrogels can be rendered completely non-degradable, degradable only by hydrolysis *or* proteolysis, or degradable by hydrolysis *and* proteolysis (**Figure 4.1**). In order to develop hypothesis towards how matrix properties play an important role in maintaining long-term cell survival in thiol-norbornene hydrogels, we evaluated (1) how hydrolytic degradation over time coupled to matrix composition i.e. macromere and crosslinker type affected matrix integrity and (2) how varying macromers (more specifically polymer molecular weight) affected matrix stiffness.
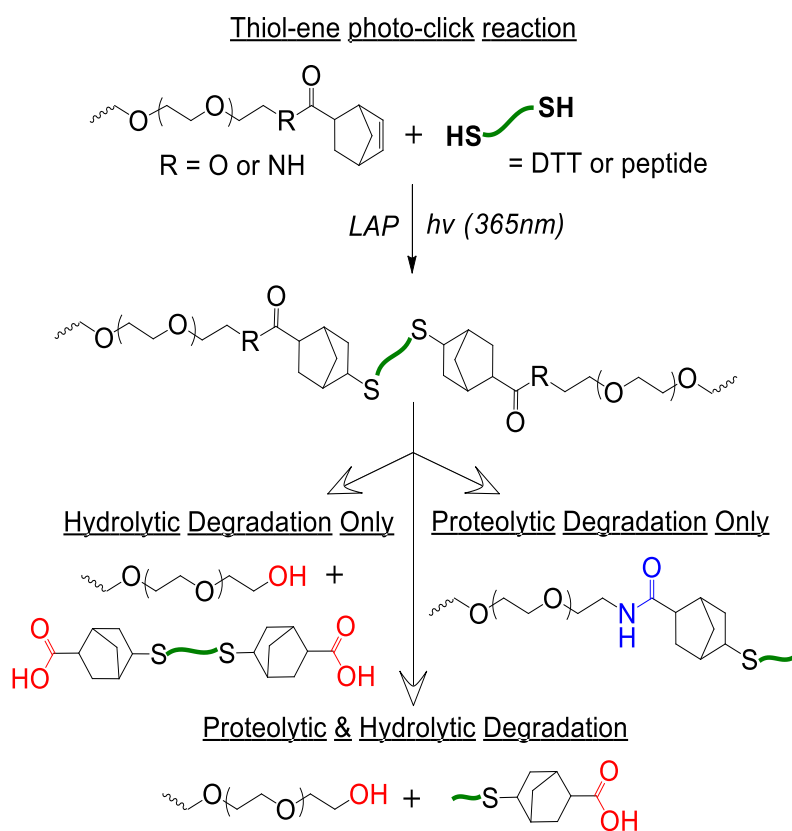
Figure 4.1. Schematic of thiol-ene photo-click reaction to form PEG-based degradable hydrogels. PEG-ester-norbornene (R = O) or PEG-amide-norbornene (R = NH) was used to construct gels with different hydrolytic degradability (only one arm of 4-arm PEG is shown). With a proper combination of macromer and cross-linker, the resulting hydrogels undergo different modes of degradation and produce different degradation products.

4.1.1 Macromer Composition and Hydrolytic Degradation of Thiol-Ene Hydrogels

To assess the effect of matrix composition and hydrolytic degradation, we synthesized two PEG-tetra-norbornene macromers with different degradability: one with hydrolytically stable amide bond (PEG4aNB (**Figure 3.1a**)) and one with hydrolytically labile ester bond (PEG4eNB (**Figure 3.1b**)). Using thiol-norbornene hydrogels cross-linked with different macromers (ester-linked PEG4eNB or amide-linked PEG4aNB) and dithiol cross-linkers (DTT, CGGYC, or KCGPQGIWGQCK (**Table 3.1**)), we performed gel swelling/degradation studies for a period of 10 days (**Figure 4.2**). The swelling/degradation profiles of thiol-ene hydrogels diverged as time due to the difference in macromer degradability and cross-linker type. Due to the presence of hydrolytically stable amide linkages, hydrogels prepared from PEG4aNB did not degrade over a period of 10 days, regardless of the cross-linkers used (**Figure 4.2**). The use of ester-linked PEG4eNB macromer, on the other hand, resulted in hydrogels with tunable hydrolytic degradation [70]. We observed that peptide (i.e., CGGYC in **Figure 4.2a** or KCGPQGIWGQCK in **Figure 4.2c**) cross-linked PEG4eNB hydrogels degraded faster compare to DTT cross-linked gels (**Figure 4.2b**). While these two peptides contained no hydrolytically labile motifs in their backbones, the presence of different amino acid side groups in the peptide cross-linkers likely accelerated the rate by which ester bonds on PEG4eNB were hydrolyzed by altering water accesibility, and hence increased the degradation rate of the hydrogels [70]. Hydrolytic degradation mechanism of PEG4eNB based hydrogels has been studied experimentally and these results were consistent with earlier reports on degradation mechanism of thiol-ene hydrogels [70].

In addition to the cross-linker chemistry, hydrogel degradability was also affected by macromer concentration. Hydrogels formed by higher macromer content (e.g., 8 wt.%) had lower initial mesh size regardless of the cross-linker used (**Figures 4.2a, 4.2b**). This phenomenon was attributed to higher network cross-linking efficiency due to higher macromer concentration [70]. Furthermore, the swelling and mesh size of hydrogels cross-linked by both macromer contents (i.e., 4 and 8 wt.%) when incubated in a buffer solution increased steadily over a period of 10 days (**Figures 4.2a, 4.2b**). It is worth

noting that gel mesh size and mechanical properties are tightly coupled and it has been proven that the two are inversely related.

When PEG4eNB was used, the resulting hydrogels had 10 to 30 % increases in gel mesh size over 10 days compared to 0 % increase when PEG4aNB was used. One would anticipate this level of degradation to play a significant role in cell fate determination in the hydrogels. Prior reports pertinent to thiol-norbornene hydrogels, however, did not evaluate the effect of this critical factor on long-term cell survival and morphogenesis.
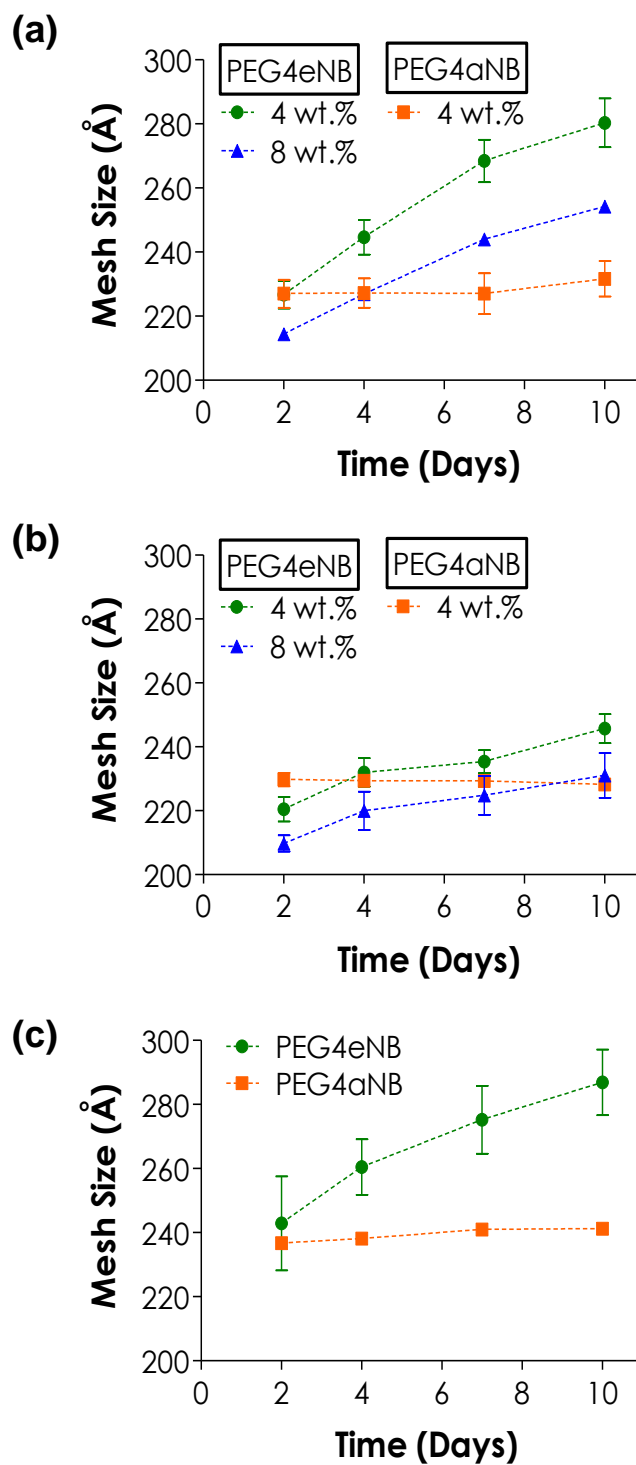
Figure 4.2. Effect of macromer compositions on mesh size (i.e., degradation) of thiol-ene hydrogels. PEG4eNB or PEG4aNB was used as macromer. Cross-linkers used were: (a) CGGYC, (b) DTT, and (c) KCGPQGIWGQCK. 4 wt% PEG macromer was used in (c) (N = 4, mean ± SD).

4.1.2 Macromer Composition and Matrix Stiffness

To evaluate the effect of matrix composition on matrix stiffness, we utilized two PEG-tetra-norbornene macromers with different molecular weights: (1) 5 kDa PEG4eNB and (2) 20 kDa PEG4eNB. Further, we crosslinked thiol-ene hydrogels using two different crosslinkers namely: DTT (not sensitive to cell secreted MMPs) and MMP$_{Linker}$ (susceptible to various cell secreted MMPs), to render gels with different matrix remodeling machanisms. After thiol-ene hydrogel formation and oscillatory rheometry (as described in **Section 3.4**), hydrogel shear moduli (G') were obtained for all experimental conditions.

The shear moduli of 5 kDa and 20 kDa PEG4eNB at equilibrium swelling states were ~5.5 kPa and ~3.1 kPa, respectively (**Figure 4.3**). The higher modulus with 5 kDa PEG4eNB can be attributed to tighter network crosslinking resulting from shorter macromer chain length compared to 20 kDa PEG4eNB macromere at the same macromere concentration [70]. Further the modulus of these gels drops over a period of 10 days due to pure hydrolytic degradation when DTT was used as crosslinker and hydrolytic and enzymatic degradation when MMP$_{Linker}$ is used (data no shown). Overall, hydrogels formed by 5 kDa PEG4eNB macromer were observed to be much stiffer than 20 kDa PEG4eNB hydrogels.

Evaluating the most relevant thiol-ene hydrogel properties i.e., hydrogel stability over time and hydrogel stiffness, will allow us to answer questions related to cell behavior over time in thiol-ene hydrogels and provide calculated hypothesis on observed cellular morphogenesis.
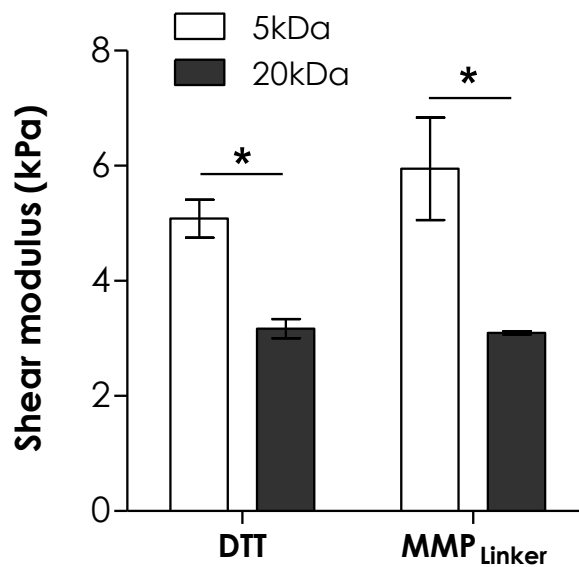
Figure 4.3. Effect of PEG4eNB macromer molecular weight on shear modulus of PEG4eNB hydrogels cross-linked by DTT or MMP$_{Linker}$ (Day-1 post-gelation, N = 4, mean ± S.D.). Asterisk represent $p < 0.05$ between indicated group.

4.2   Investigating the Survival and Proliferation of Pancreatic Beta Cells and Human
Mesenchymal Stem Cell in 3D

To understand the influence of thiol-ene hydrogel properties on cellular morphogenesis, cells derived from both epithelial tissue (e.g, pancreatic MIN6 β-cells) and mesenchymal tissues (e.g., human mesenchymal stem cells or hMSCs) were used in this study. First, the effects of thiol-ene reaction conditions on initial and long-term cell survival following photo-encapsulation were studied using various techniques. Second, in view of the importance of cell-mediated matrix remodeling on survival and differentiation of hMSCs, we incorporated a matrix metalloproteinase (MMP) sensitive peptide (MMP$_{Linker}$) as the cross-linker in thiol-ene hydrogels to render the gels proteolytically degradable. Finally, a fibronectin-derived cell adhesive ligand, Arg-Gly-Asp-Ser or RGDS, was conjugated within the otherwise inert PEG-based hydrogels to illustrate the cooperative influence of gel degradation and cell-matrix interactions on cell survival and spreading.

4.2.1   Effect of Macromer Composition on Cell Viability Following *In Situ* Photo-Encapsulation

To understand the effect of thiol-norbornene hydrogel properties on cell survival and morphogenesis, it is important to examine the initial cell viability following *in situ* gelation and encapsulation.   Thus, immediately following photo-encapsulation we assessed the viability of the encapsulated cells qualitatively using Live/Dead staining and quantitatively with CellTiter Glo® reagent.   We found that increasing macromer concentration from 4 to 8 wt.% decreased viability of encapsulated MIN6 β-cells from 85 ± 3 % to 71 ± 4 % in CGGYC cross-linked PEG4eNB hydrogels, and from 85 ± 1 % to 75 ± 3 % in DTT cross-linked PEG4eNB hydrogels (**Figures 4.4a, 4.4b**). Similar reduction in initial cell viability at higher macromer content was also found in encapsulated hMSCs (**Figures 4.5a, 4.5b**). The effect of macromer concentration and cross-linker type on initial cell viability was also assessed quantitatively by intracellular ATP measurements for both MIN6 β-cells (**Figure 4.4c**) and hMSCs (**Figure 4.5c**). These ATP assays were conducted one-hour post-encapsulation and the results correlated

directly to the number of metabolically active cells following photo-encapsulation. Not surprisingly, these quantitative results agree with the qualitative images shown in **Figure 4.4 and 4.5**, confirming the negative influence of high functional group concentrations on cell survival during and following photoencapsulation.
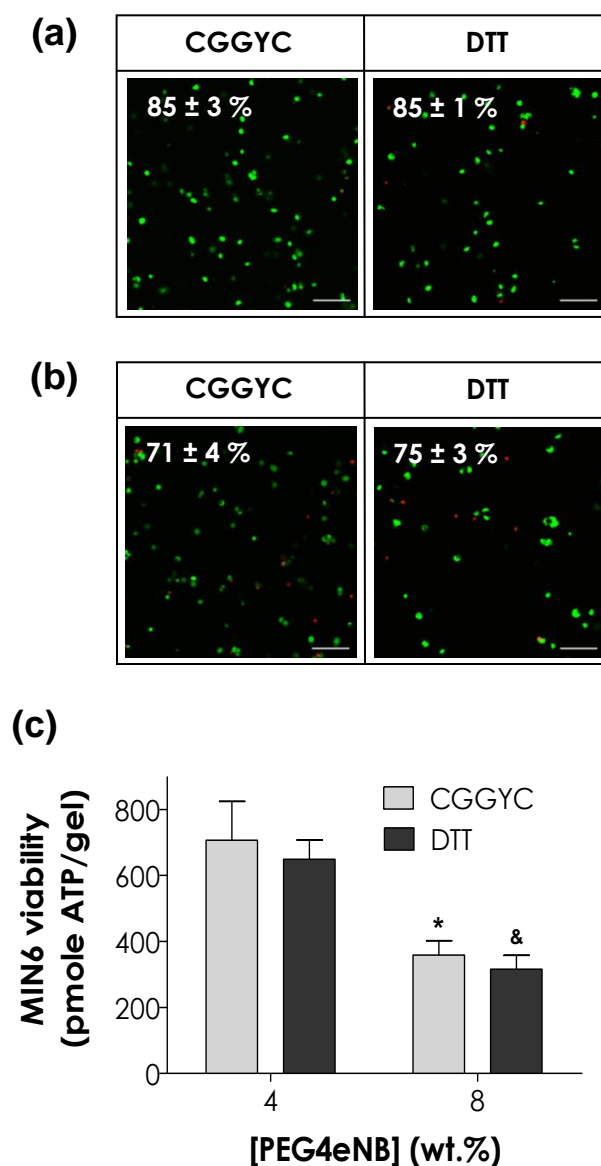
Figure 4.4. Effect of hydrogel formulation on initial viability of MIN6 β-cells encapsulated in (a) 4 wt% or (b) 8 wt% PEG4eNB hydrogels cross-linked by different linker (CGGYC or DTT as indicated). (a, b) Cell-laden hydrogels were stained with Live/Dead staining kit and imaged with confocal microscope. Numbers shown in the representative confocal z-stack images were the percentages of live cells over total cell count (Scale: 100μm; N = 4, mean ± S.D.). (c) Intracellular ATP concentrations were determined by Cell-Titer Glo® reagent 1 hour post-encapsulation. (N = 4, mean ± SD). Asterisk and ampersand represent p < 0.05 within respective group (i.e., compared to 4 wt% gels).

Collectively, the decreased initial cell viability at higher macromer concentrations could be attributed to: (1) higher concentrations of radical species generated during network cross-linking and (2) higher degree of cross-linking at higher macromer concentrations. It has been shown that cells are sensitive to radical species generated during photopolymerization reaction [27]. When macromer concentration was raised from 4 to 8 wt.%, the total functionality (i.e., thiol and norbornene groups) in the pre-polymer solution was increased by 100 % from 16 to 32 mM. This drastic increase in macromer functionality resulted in higher radical concentration and higher extent of thiol-norbornene click reaction [59, 70], both of which may contribute to decreased initial cell viability. Additionally, increased macromer content in the pre-polymer solution led to a higher network cross-linking density [70, 93], and hence caused higher degree of environmental stresses that could negatively affect initial cell survival. For all macromer concentrations used, however, we did not observe significant differences in cell viability between gels formed by different macromer type (i.e., PEG4eNB or PEG4aNB) or cross-linkers (i.e., DTT or CGGYC). This could be attributed to the fact that, at the same functional group concentration, changing the type of cross-linker or macromer does not cause significant differences in the degrees of thiol-norbornene reaction and network cross-linking.
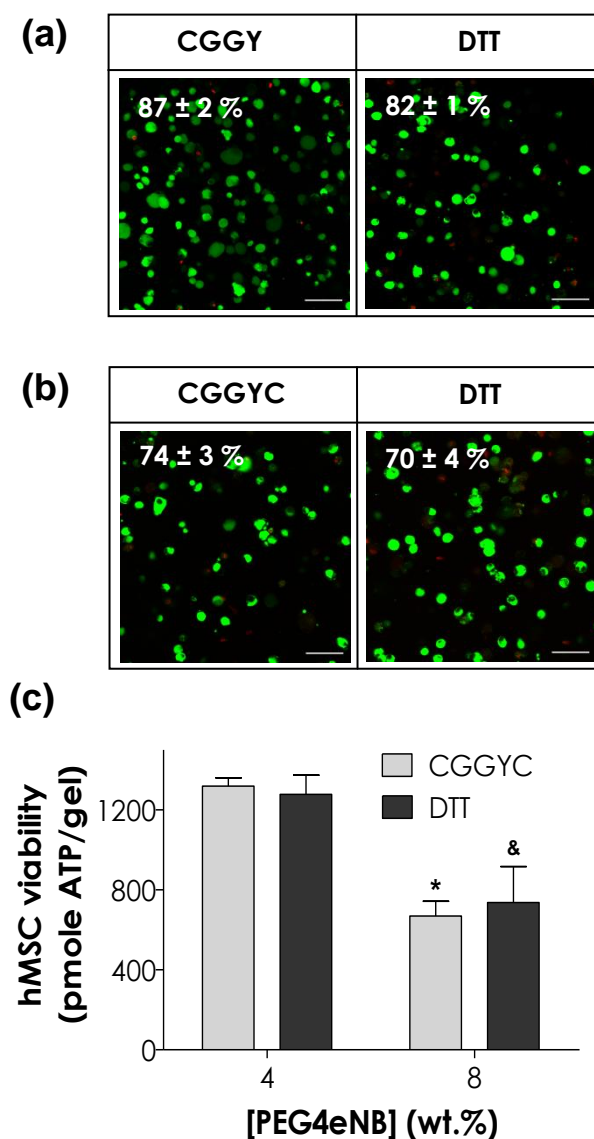
Figure 4.5. Effect of hydrogel formulation on initial viability of hMSCs encapsulated in (a) 4 wt% or (b) 8 wt% PEG4eNB hydrogels cross-linked by different linker (CGGYC or DTT as indicated). (a, b) Cell-laden hydrogels were stained with Live/Dead staining kit and imaged with confocal microscope. Numbers shown in the representative confocal z-stack images were the percentages of live cells over total cell count (Scale: 100μm; N = 4, mean ± S.D.). (c) Intracellular ATP concentrations were determined by Cell-Titer Glo® reagent 1 hour post-encapsulation. (N = 4, mean ± SD). Asterisk and ampersand represent p < 0.05 within respective group (i.e., compared to 4 wt% gels).

While the initial viability decreased with increasing macromer concentration, most of the cells survived the photo-encapsulation process ($\sim 70 - 90$ %), even at low cell packing densities. Previous studies have demonstrated that only about 40 % of the encapsulated β-cells survived following photoencapsulation in chain-growth PEGDA hydrogels at a cell packing density of 6.7×10^6 cells/mL and essentially no cell survived when the cell packing density was lower than 5×10^6 cells/mL [55]. A previous study has also shown that only about 77 % of the encapsulated hMSCs survived a UV-based chain-growth PEGDA photoencapsulation process, with an extremely high cell packing density of 25×10^6 cells/mL [94]. Taken together, step-growth thiol-norbornene photo-click chemistry affords milder reaction conditions that preserve the viability of cells from either epithelium (pancreatic β-cells) or mesenchyme (hMSCs) origin.

4.2.2   Effect of Hydrolytic Gel Degradation on Long-Term Cell Viability

Previously we have shown that PEG hydrogels formed by thiol-norbornene photo-click reactions supported the formation of MIN6 β-cells spheroids in 3D [27]. Using thiol-norbornene hydrogels with identical macromer chemistry, Anderson *et al.* showed that proteolytic degradation in gels supported the survival and differentiation of hMSCs [92]. These reports did not, however, examine the influence of hydrolytic degradation in thiol-norbornene hydrogels on the observed cell behaviors. We hypothesized that hydrolytic degradation in the ester-containing PEG4eNB macromer has beneficial effects on long-term viability for both epithelial (e.g., MIN6) and mesenchymal (e.g., hMSCs) cell types. To prove this, we assessed the viability of encapsulated MIN6 β-cells and hMSCs qualitatively using Live/Dead staining (**Figure 4.6a – 4.6c, 4.8a – 4.8c**) and quantitatively using AlamarBlue® reagent (**Figure 4.6d, 4.6e, 4.8d, 4.8e**).

We found that the majority of cells survived in all gel formulations tested over a period of 10 days (**Figure 4.6, 4.8**). As expected, MIN6 β-cells formed spherical aggregates (**Figures 4.6a – 4.6c**) while hMSCs retained their round and dispersed morphology (**Figures 4.8a – 4.8c**) in all hydrogels. The degree of cell survival and/or

proliferation, however, decreased significantly in gels with slower (e.g., DTT-crosslinked) or no hydrolytic degradation (e.g., PEG4aNB-based). For example, PEG4eNB hydrogels crosslinked by CGGYC supported the formation of larger spheroids compared to using DTT as crosslinker (45 ± 1 vs. 39 ± 1 μm, **Figures 4.6a, 4.7**). Moreover, MIN6 β-cell spheroids formed in non-degradable PEG4aNB hydrogels, regardless of the crosslinkers used, appeared much smaller (~ 21 μm) compared to the hydrolytically degradable gels (**Figures 4.6c, 4.7**). Quantitative cell proliferation assay agrees with the qualitative Live/Dead staining. For example, the degree of MIN6 β-cells proliferation in 4 wt.% CGGYC-cross-linked hydrogels dropped from ~580 % to ~220 % when PEG4eNB macromer was replaced by PEG4aNB (**Figure 4.6d**). Further, the use of higher PEG macromer content (e.g., 8 wt.%) or DTT as a gel cross-linker (**Figure 4.6d, 4.6e**) significantly hindered MIN6 β-cell proliferation.
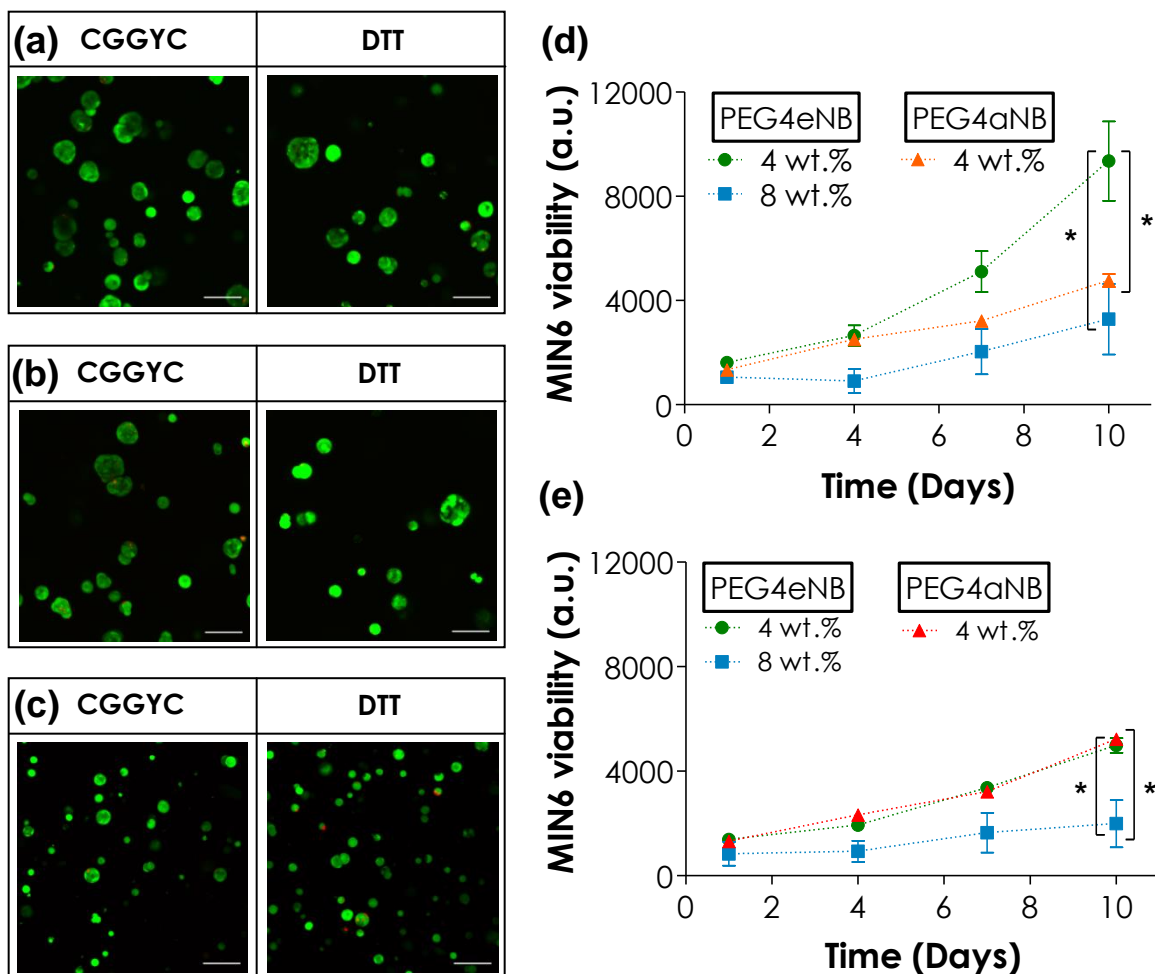
Figure 4.6. Effect of hydrogel formulation on sustaining MIN6 β-cells survival and proliferation. (a – c) Cell-laden hydrogels were stained with Live/Dead staining kit and visualized by confocal microscopy (z-stack images) at day 10. Macromer used: (a) 4 wt% PEG4eNB, (b) 8 wt% PEG4eNB, and (c) 4 wt% PEG4aNB thiol-ene hydrogels (Scale: 100μm). (d , e) Cell viability as time was determined quantitatively by AlamarBlue® reagent. Linker type: (d) CGGYC, (e) DTT (N = 3, mean ± SD). Asterisk represent $p < 0.05$ between indicated group.

While MIN6 β-cells formed spheroids in all gel formulations, encapsulated hMSCs remained round and single cell morphology in these gels (**Figures 4.8a – 4.8c**). The morphological differences in epithelial and mesenchymal cells in 3D have been reported in numerous other publications [92, 95-98]. What has not been shown is the profound impact of hydrolytic degradation in thiol-ene hydrogels on the survival of hMSCs in 3D. For instance, hMSCs encapsulated in higher 8 wt.% PEG4eNB gels (**Figure 4.8b**) or non-degradable PEG4aNB gels (**Figure 4.8c**) suffered from higher degree of cell death and appeared slightly smaller in cell size, especially in DTT-cross-linked gels. Quantitative viability assay showed that hMSCs encapsulated in degradable PEG4eNB (4 wt.%) gels cross-linked by CGGYC roughly maintained their viability throughout the 10-day culture period (**Figure 4.8d**). Unfortunately, cell viability dropped almost monotonically as time in gels that degraded slowly (DTT-cross-linked) or lacking significant hydrolytic degradation (with PEG4aNB) (**Figure 4.8e**). The positive correlation between cell survival and/or proliferation (**Figures 4.6, 4.8**) and thiol-norbornene hydrogel degradation (**Figure 4.2**) suggest that hydrolytic degradation in the hydrogel matrix plays an important role in promoting cell viability in 3D.

(a)

(b)
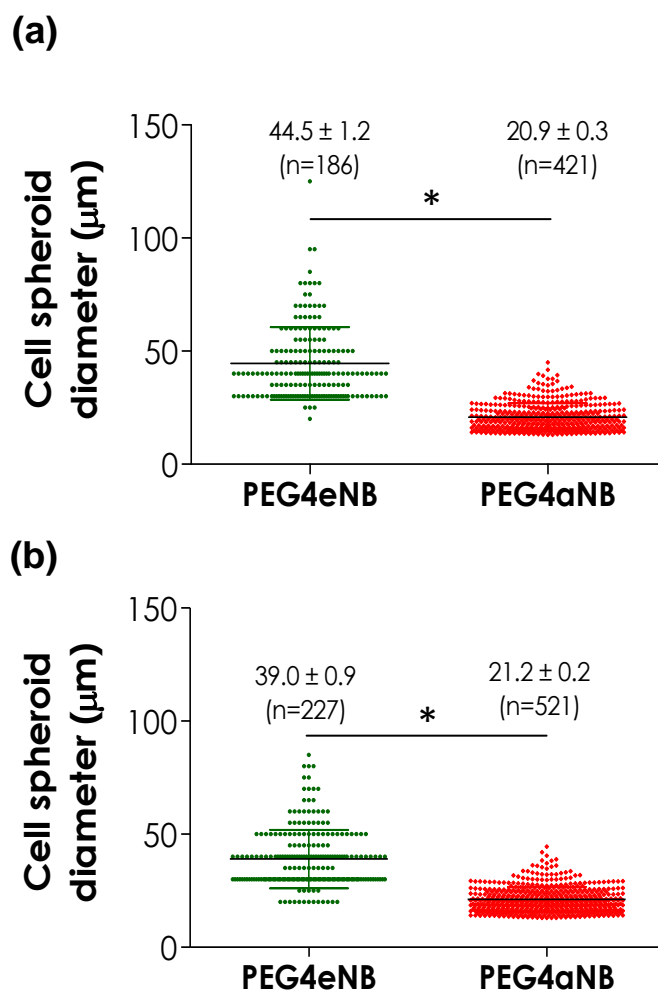
Figure 4.7. Diameter distribution of MIN6 β-cell spheroids formed in 4 wt.% PEG4NB hydrogels cross-linked by (a) CGGYC or (b) DTT. (Day-10, N = 4, mean ± SD). Asterisk represent p < 0.05 within indicated group.
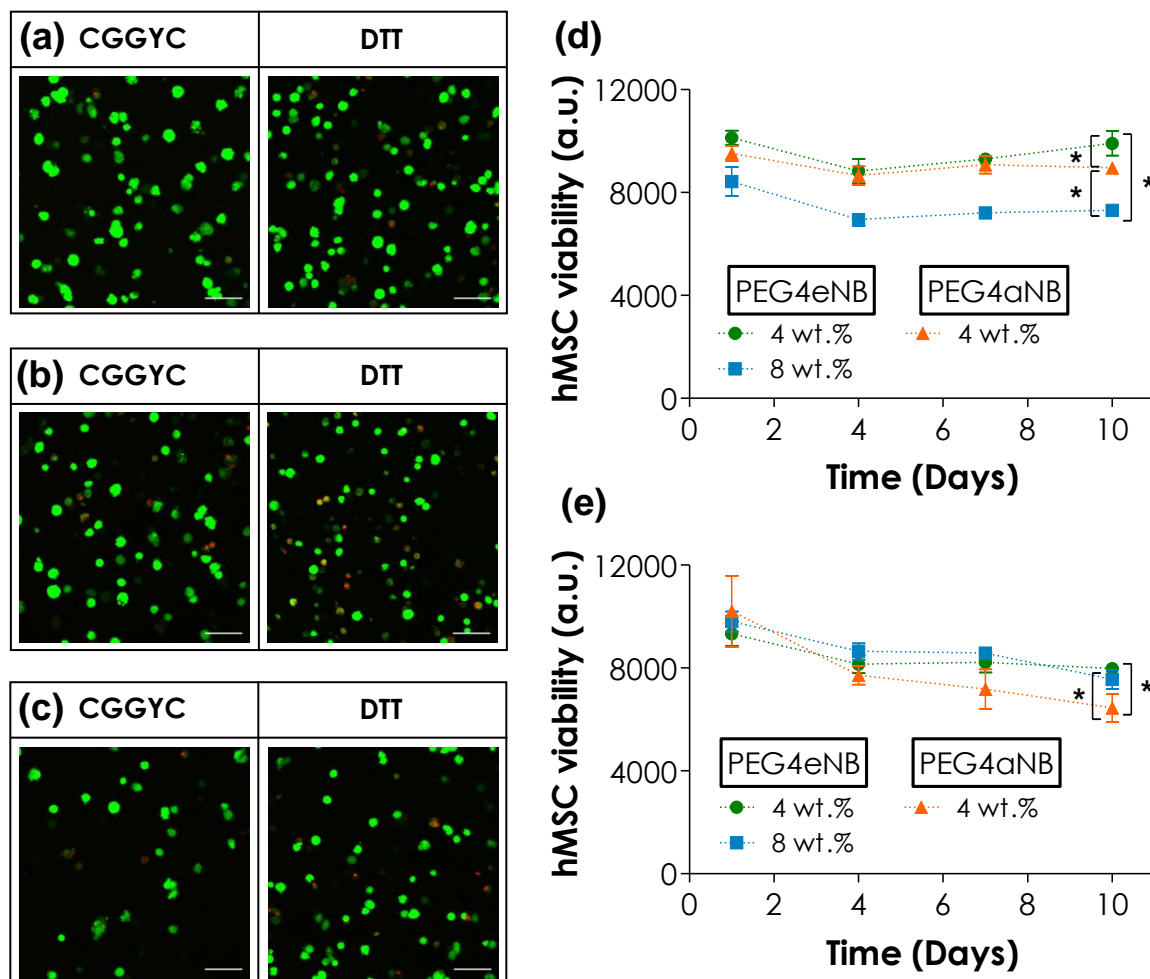
Figure 4.8. Effect of hydrogel formulation on sustaining hMSCs survival and proliferation. (a – c) Cell-laden hydrogels were stained with Live/Dead staining kit and visualized by confocal microscopy (z-stack images) at day 10. Macromer used: (a) 4 wt% PEG4eNB, (b) 8 wt% PEG4eNB, and (c) 4 wt% PEG4aNB thiol-ene hydrogels (Scale: 100μm). (d , e) Cell viability as time was determined quantitatively by AlamarBlue® reagent. Linker type: (d) CGGYC, (e) DTT (N = 3, mean ± SD). Asterisk represent $p < 0.05$ between indicated group.

Further, phenotypic evaluation was performed on both encapsulated MIN6 β-cells and hMSCs using whole mount immunostaining. MIN6 β-cells and hMSCs were stained for insulin and CD105, respectively after 10 days of culture in thiol-ene hydrogels. Results obtained via confocal microscopy, confirmed that both cells types remain undifferentiated and express there phenotypic proteins i.e., MIN6 β cells express insulin (**Figure 4.9a**) and hMSCs express CD105 (**Figure 4.9b**). These results provide further evidence that thiol-ene hydrogels not only provides a cytocompatible microenvironment for cells but also provide an unbiased blank slate environment for long-term preservation and culture of cells.

(a)

Insulin	Combined
MIN6	

Insulin/DAPI

(b)

CD105	Combined
hMSC	

CD105/DAPI
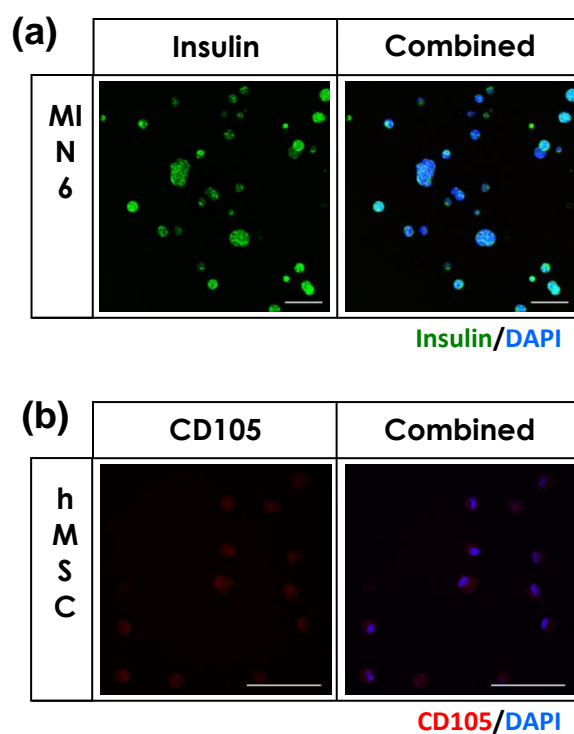
Figure 4.9. Representative z-stack immunostaining images of (a) MIN6 β-cells and (b) hMSCs. Cells were stained using antibodies targeting (a) insulin (green) and (b) CD105 (red) 10 days post encapsulation in 4 wt.% PEG4eNB/CGGYC hydrogels. Cell nuclei were counter stained with DAPI (blue). (Scale: 100μm)

4.2.3 Effect of Cell-Adhesive Motif and Hydrolytic Gel Degradation on Long-Term Cell Viability

It should be noted that results shown in **Figures 4.4** through **4.8** were obtained from PEG-based hydrogels without the presence of bioactive moieties, which have proven beneficial in supporting cell survival in 3D [46, 99, 100]. Toward this end, we were interested in illustrating the potential synergistic influence of gel hydrolytic degradation and cell-adhesive motifs, such as fibronectin-derived RGDS on cell survival and morphogenesis. We monitored the viability of MIN6 β-cells and hMSCs encapsulated in CGGYC cross-linked hydrogels (PEG4eNB or PEG4aNB) incorporated with 0, 1, and 2 mM of CRGDS. At the peptide concentrations tested, the incorporation of RGDS motif only marginally increased viability of MIN6 β-cells in hydrolytically degradable PEG4eNB hydrogels at day-10 (**Figures 4.10a**). On the other hand, a higher degree of pro-survival effect afforded by RGDS can be seen at day-7 onward when non-degradable PEG4aNB macromer was used (**Figures 4.10b**). The influence of RGDS motif on cell survival was more apparent in encapsulated hMSCs. For example, hMSCs encapsulated in thiol-ene hydrogels immobilized with 1 mM or 2 mM RGDS consistently showed higher viability at all-time points, regardless of hydrogel degradability (**Figures 4.11a**, **4.11b**). The promoting effect of RGDS peptide in cell viability was significantly higher in non-degradable PEG4aNB hydrogels (**Figure 4.11b**), compared to cell viability in hydrolytically degradable PEG4eNB hydrogels (**Figure 4.11c**). We believe that, in the case where thiol-ene gels were susceptible to hydrolytic degradation, the encapsulated cells were relieved from polymer network stresses as time and consequently the role of RGDS motif became less significant. Murphy and colleagues have previously reported similar behaviors in hMSCs encapsulated in hydrolytically degradable Michael-type PEG hydrogels [99-101]. When the gels were not hydrolytically degradable (i.e., using amide-linked PEG4aNB), the inclusion of RGDS potentially rescued the cells from damages by providing critical cell-matrix interactions that were otherwise lacking (**Figures 4.11b, 4.11b**).

(a)

(b)
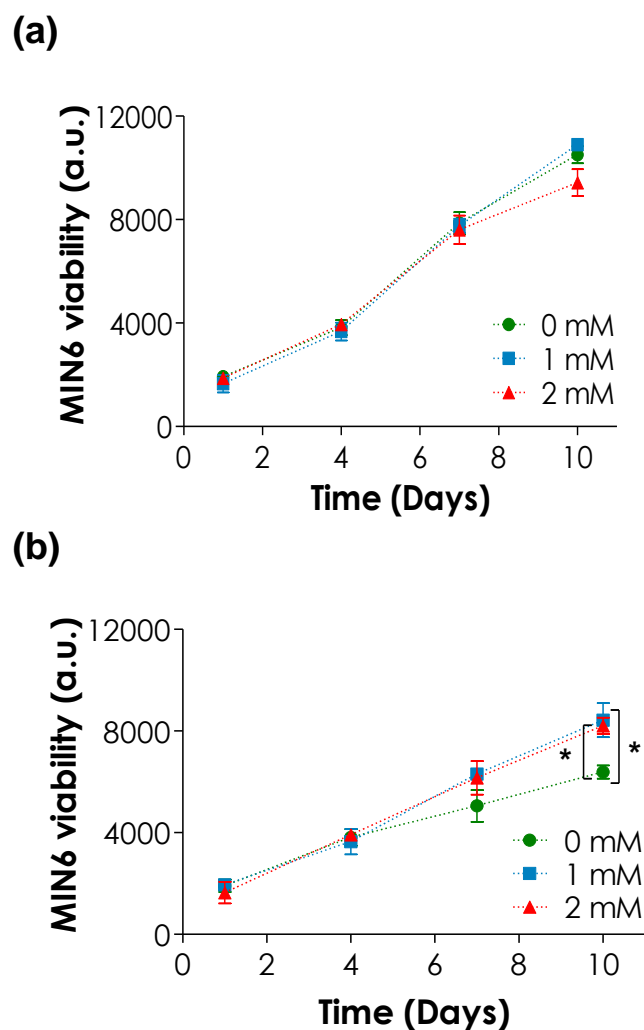
Figure 4.10. Effect of cell-matrix interaction on sustaining survival and proliferation of MIN6 β-cells. Cell viability as time was determined quantitatively by AlamarBlue® reagent. Cells were encapsulated in 4 wt.% (a) PEG4eNB or (b) PEG4aNB hydrogels crosslinked by CGGYC with varying concentrations of immobilized CRGDS. (N = 3, mean ± SD). Asterisk represent $p < 0.05$ between indicated group.

(a)

(b)
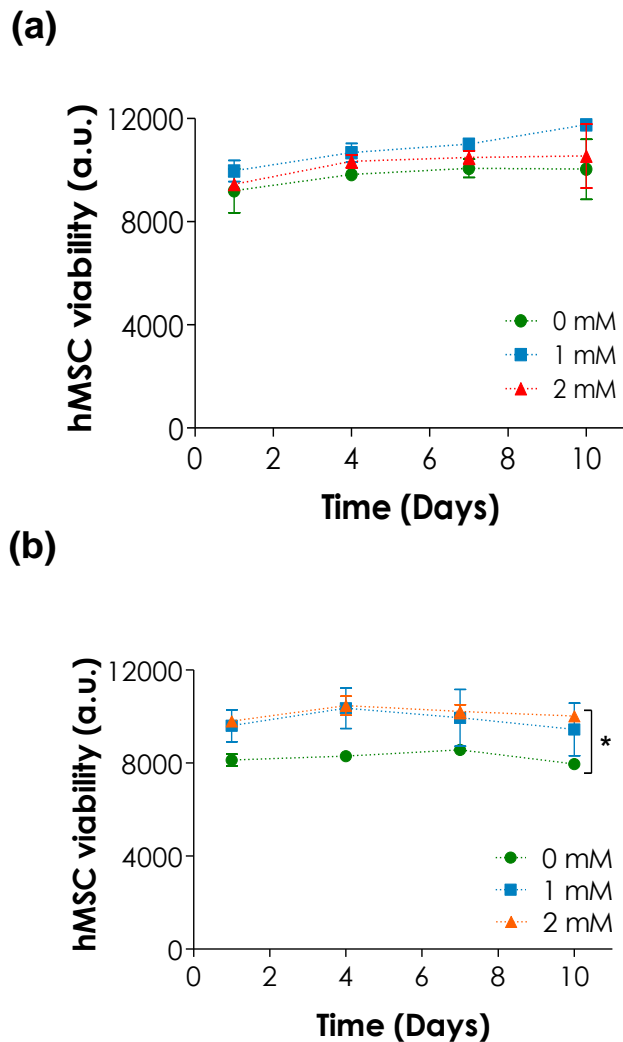
Figure 4.11. Effect of cell-matrix interaction on sustaining survival and proliferation of hMSCs. Cell viability as time was determined quantitatively by AlamarBlue® reagent. Cells were encapsulated in 4 wt.% (a) PEG4eNB or (b) PEG4aNB hydrogels crosslinked by CGGYC with varying concentrations of immobilized CRGDS. (N = 3, mean ± SD). Asterisk represent $p < 0.05$ between indicated group.

4.2.4 Effect of Hydrolytic Gel Degradation, Cell-Mediated Matrix Remodeling, and Cell-Matrix Interaction on hMSC Viability and Morphology

An attractive feature of thiol-ene hydrogels is that the gels can be designed to undergo cell-mediated matrix remodeling by using protease (e.g., MMPs) sensitive peptides as gel cross-linkers [63]. Selective cleavage of matrix locally by cell-secreted proteases alters the extent to which the cells interact with their microenvironment. Furthermore, the degree of cell spreading due to local matrix degradation has been shown to significantly impact cell fate determination [92, 102]. For example, Anderson *et al.* showed that the degree of proteolytic degradation in thiol-ene hydrogels significantly affected the survival, proliferation, and differentiation of hMSCs [92]. Given the profound impact of gel hydrolytic degradation on cell survival as shown in **Figures 4.6** through **4.8**, we reasoned that these two forms of gel degradation (i.e., proteolytic and hydrolytic) might collaboratively affect hMSCs morphology and survival under the influence of cell-matrix interactions (provided by immobilized integrin ligand, RGDS).

To evaluate this possibility, we encapsulated hMSCs in PEG4eNB or PEG4aNB hydrogels crosslinked by an MMP-sensitive peptide linker (i.e., KCGPQG↓IWGQCK) incorporated with 0, 1, and 2 mM of CRGDS. We characterized cell morphology qualitatively using Live/Dead staining, f-actin immunostaining and confocal imaging (**Figure 4.12, 4.13**) while measured cell viability quantitatively using AlamarBlue® reagent (**Figure 4.14**). Without RGDS motif, the morphology of hMSCs encapsulated in MMP-sensitive peptide cross-linked hydrogels (**Figure 4.12a**) appeared similar to that found in CGGYC or DTT cross-linked gels (**Figures 4.8d – 4.8e**). This result demonstrates the importance of integrin-binding on cell-mediated matrix remodeling.

Similar to the results shown by Anderson *et al.*, hMSCs exhibited extensive cellular processes only when they were encapsulated in an MMP-sensitive microenvironment *and* in the presence of RGD motif (**Figure 4.12b, 4.12c**). Interestingly, however, the percentage of cells exhibiting long cellular processes due to enhanced cell-matrix interaction was significantly higher in hydrolytically labile PEG4eNB-based hydrogels than in hydrolytically stable PEG4aNB-based gels (**Figures**

4.12b – 4.12e, 4.13). For example, over 90 % of cells in degradable PEG4eNB hydrogels had cellular processes longer than 30 μm compared to only ~50 % of the cells in non-degradable PEG4aNB hydrogels cross-linked by the same MMP-sensitive peptide and immobilized with 1 mM RGDS (**Figure 4.12d**). The analysis of cell average lengths in these hydrogels yielded a similar trend (**Figure 4.12e**). For example, when hMSCs were encapsulated in PEG4eNB hydrogels immobilized with 1 mM RGDS, the average cell length was ~80 μm, as compared to only ~47 μm in PEG4aNB hydrogels. Increasing the concentration of immobilized RGDS to 2 mM did not yield significant differences in the percentage of cells exhibiting long protrusions or the average cell lengths. When comparing the morphology of hMSCs encapsulated in PEG4eNB or PEG4aNB hydrogels immobilized with 2 mM RGDS, the differences between the percentages of cells exhibiting long processes and the average cell lengths decreased as compared to those found in 1 mM RGDS containing gels. It is important to note that all of these hydrogels were cross-linked by the same MMP-sensitive peptide. The hydrolytic degradation of PEG4eNB hydrogels likely enhanced cell-matrix interactions that led to higher degree of cell spreading. This phenomenon suggested that hydrolytic gel degradation could be exploited to achieve a similar level of intracellular signaling at a lower concentration of bioactive motif.

While hMSCs encapsulated in gels cross-linked by CGGYC or DTT barely survived at longer 3D culture time (**Figures 4.8**), we found that hydrolytic degradation enhanced cell viability (measured by Alamarblue® reagent) in gels cross-linked by MMP-sensitive linker even without the presence of RGDS (**Figure 4.14a**). This trend holds when 1 mM of RGDS was incorporated (**Figure 4.14b**) but the difference in cell viability between the two macromers (PEG4eNB and PEG4aNB) diminished when the concentration of immobilized RGDS was raised to 2 mM (**Figure 4.14c**). This was similar to the trend observed in the 3D spreading of hMSCs as shown in **Figure 4.13**. Collectively, these results suggest that hydrolytic degradation, proteolytic degradation, and cell-matrix interactions work together in enhancing cell performance in PEG-based thiol-ene hydrogels.
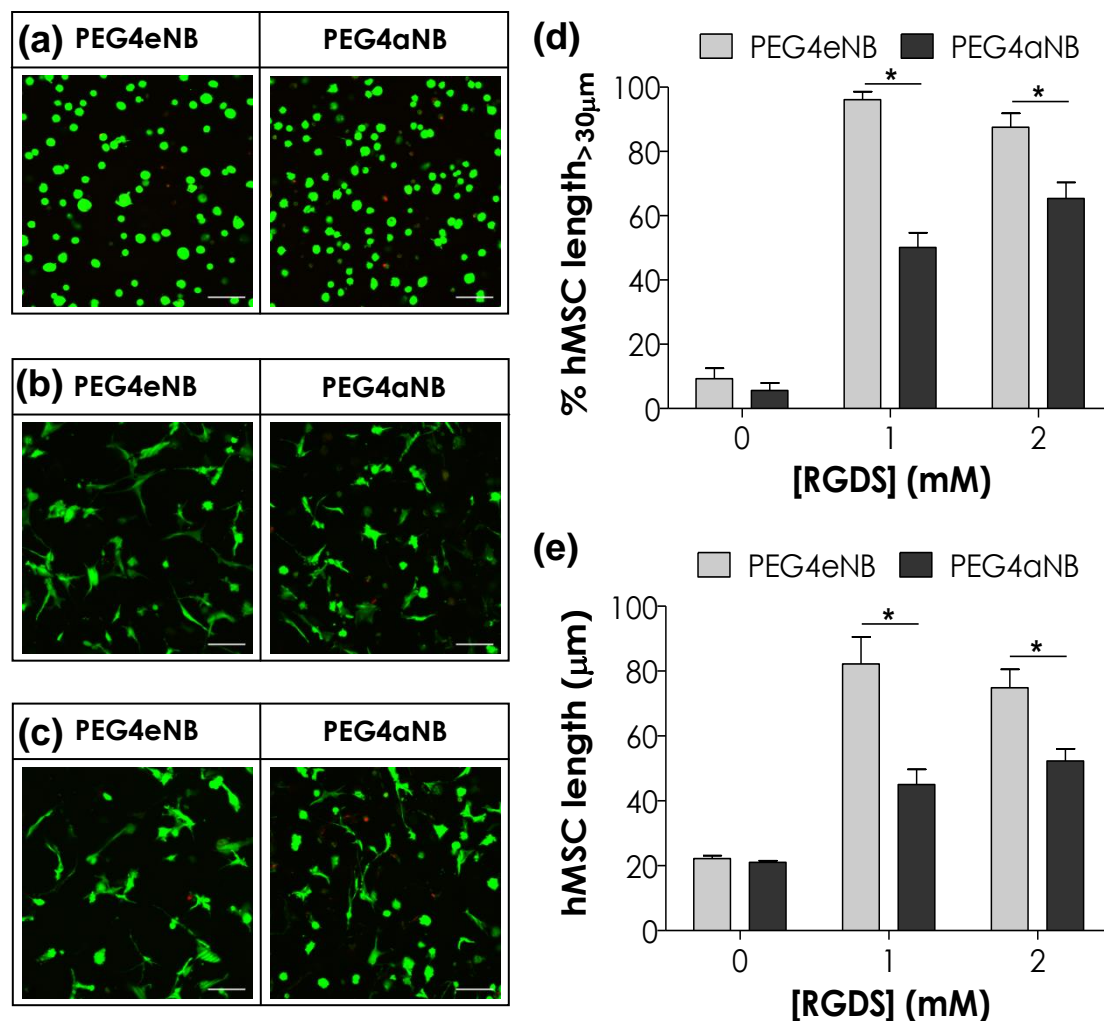
Figure 4.12. Effect of hydrogel degradation and cell-matrix interaction on hMSC morphology. (a – c) Cell-laden hydrogels were stained with Live/Dead staining kit after 10 days of culture. Representative confocal z-stack images of hMSCs encapsulated in 4 wt.% PEG-norbornene hydrogels crosslinked by MMP_{Linker} and immobilized with (a) 0 mM, (b) 1 mM, and (c) 2 mM of CRGDS (Scale: 100µm). (d) Image analysis results showing % of hMSCs having cell length of 30 µm or longer. (e) Image analysis results showing the average cell lengths of encapsulated hMSCs (N = 4, mean ± S.D.). Asterisk represent p < 0.05 within indicated group.

Independent evaluation of epithelial and mesenchymal morphogenesis using MIN6 β-cells and hMSCs, respectively, have revealed key matrix properties including: initial reaction conditions, macromer composition, hydrogel degradability and hydrogel bioactivity, to maintain and study long term cellular morphogenesis in 3D.
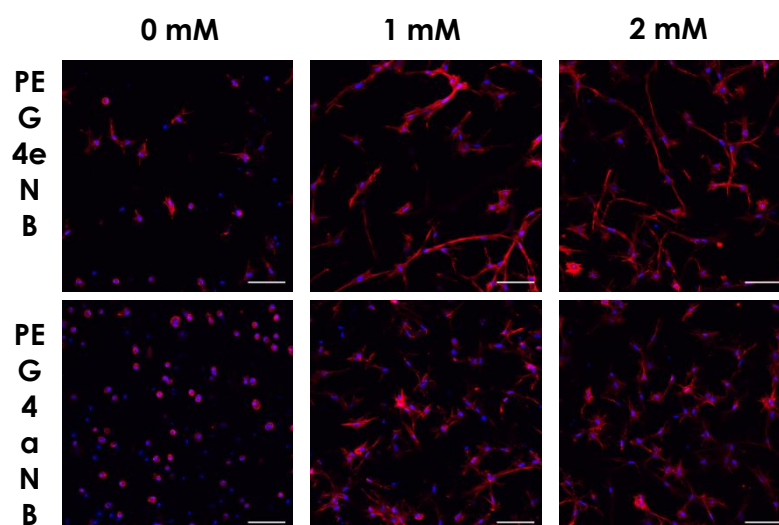
Figure 4.13. Effect of hydrogel degradation and cell-matrix interaction on hMSC morphology 10 days post-encapsulation. Representative confocal z-stack immunostaining images of hMSCs stained with Rhodamine-labeled Phalloidin for f-actin (red). Cell nuclei were counter stained with DAPI (blue). Cells were encapsulated in 4 wt.% PEG4NB hydrogels crosslinked by MMP$_{Linker}$ and immobilized with 0 mM,1 mM, and 2 mM of CRGDS. (Scale: 100μm)
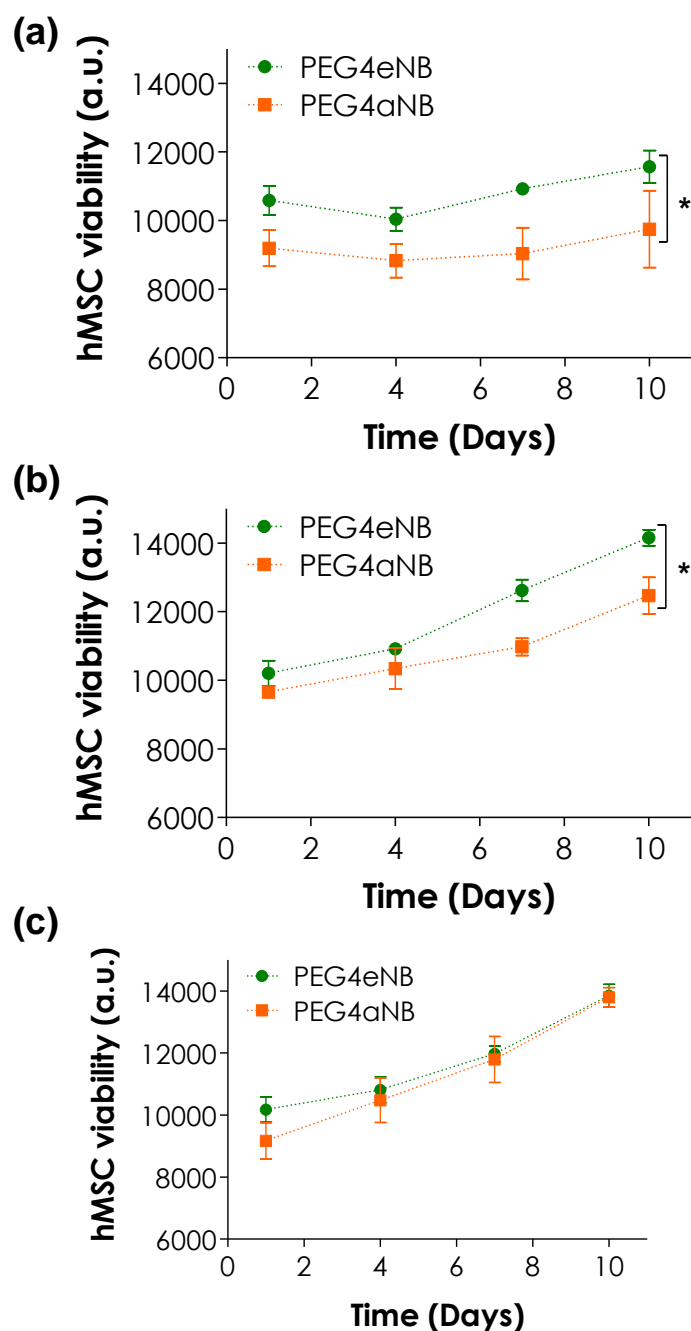
Figure 4.14. Effect of hydrogel degradation and cell-matrix interaction on sustaining hMSC survival and proliferation. hMSCs were encapsulated in 4 wt.% PEG-norbornene hydrogels crosslinked by MMP_{Linker} and immobilized with (a) 0 mM, (b) 1 mM, or (c) 2 mM of CRGDS. Viability as time was determined by AlamarBlue® reagent (N = 3; Mean ± S.D.). Asterisk represent $p < 0.05$ within indicated group.

4.3   EstablishingTunable Hydrogel Niches for Culturing Pancreatic Exocrine Cells

Unlike MIN6 β-cells and hMSCs, PANC-1 cells have not been comprehensively studies in 3D. This creates a need to evaluate the behavior of these cells in 3D and further the understanding towards epithelial – mesenchymal morphogenesis. Towards this end, thiol-ene hydrogel matrix was manipulated at: (1) *cross-linker level* to explore the effect of different rates and modes of degradation on PANC-1 cellular morphogenesis, (2) *macromer molecular weight level* to evaluate the effect of stressful microenvironment on cellular behavior, and (3) *cell–ECM interaction level* to observe the changes in PANC-1 cell morphogenesis due to ECM interaction. Matrix adjustments at these levels will allow us to study the independent and synergistic effect of various matrix conditions on cell morphogenesis. For all the studies performed in this section 5 wt.% PEG4eNB thiol-ene hydrogels were utilized to encapsulate PANC-1 cells.

4.3.1   Effect of Macromer Composition on Initial PANC-1 Viability

As discussed previously, most studies performed on PANC-1 cell have been in 2D culture and that only on a few occasions PANC-1 cell features in comparison to other cell lines have been evaluated in 3D culture [79, 85, 103, 104]. To explore PANC-1 morphogenesis in thiol-ene hydrogels, we first examined the initial cell viability immediately following photoencapsulation. We assessed the viability of encapsulated PANC-1 cells at cell packing density of 2×10^6 cell/mL 1 hour post *in situ* gelation in 5 wt.% 20 kDa PEG4eNB hydrogels with varying cross-linker type qualitatively using Live/Dead staining and quantitatively with CellTiter Glo® reagent (**Figure 4.15**).

(a)

(b)
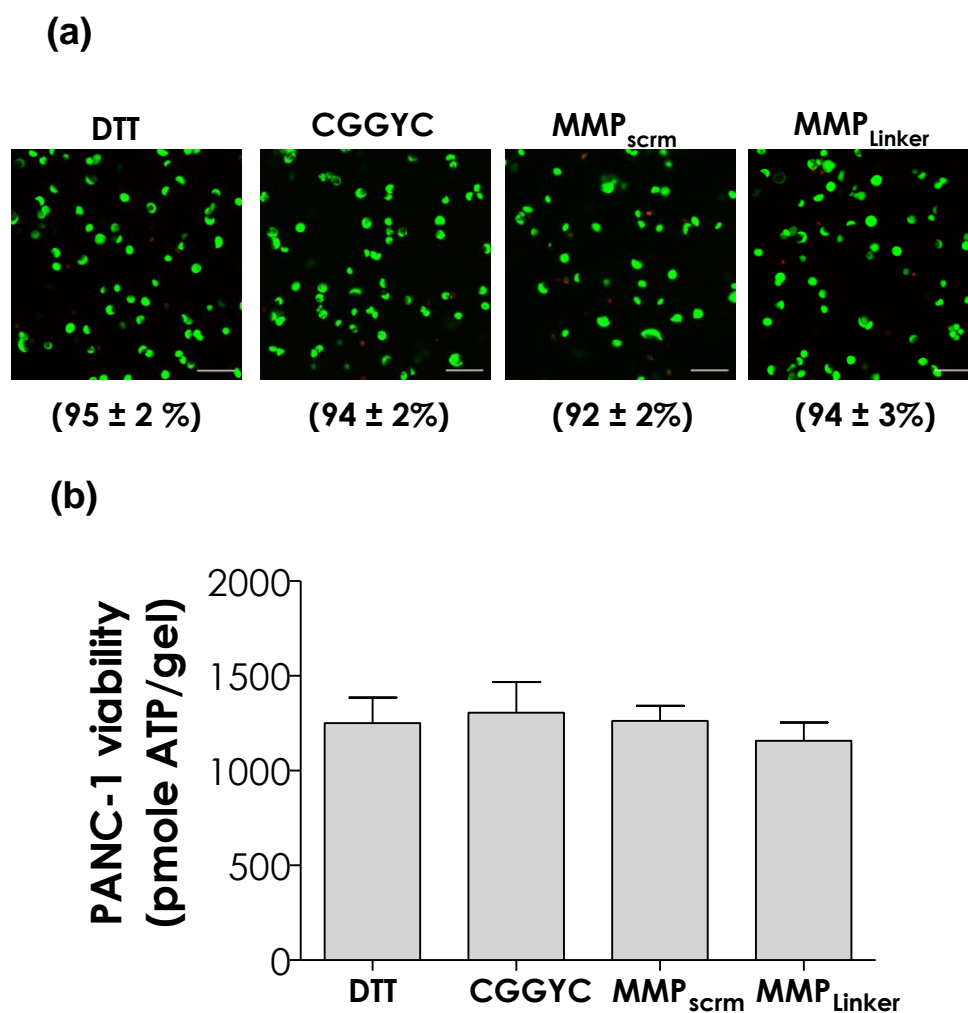
Figure 4.15. Effect of cross-linker chemistry on initial viability of photoencapsulated PANC-1 cells (5 wt% PEG4NB). (a) Representative confocal z-stack images of PANC-1 cells stained with Live/Dead staining kit. Numbers shown below each image represent the percentage of live cells over total cell count (Scale: 100μm; N = 4, mean ± S.D.). (b) Quantitative cell viability (one hour post-encapsulation) determined by CellTiter Glo® reagent that measures intracellular ATP concentration. No statistical significant difference was found between any two groups (N = 4, mean ± SD).

We found that varying crosslinker had no significant effect on initial viability of encapsulated PANC-1 cells i.e., in all crosslinker formulations over 90% of cells survived the photoencapsualtion process as observed by Live/Dead staining (**Figure 4.15a**). The effect of cross-linker type on initial cell viability was also assessed quantitatively by intracellular ATP measurements (**Figure 4.15b**). These ATP assays results correlated directly to the number of metabolically active cells following photo-encapsulation and the results agree with the qualitative Live/Dead images as shown in **Figure 4.15**. These results could be attributed to the fact that, at the same functional group concentration, changing the type of cross-linker does not cause significant differences in the degrees of thiol-norbornene reaction and network cross-linking. These initial viability results show that thiol-ene chemistry support high degree of cell survival during and following photoencapsulation.

We further evaluated the effect of PEG4eNB macromer molecular weight (M.W.) on initial PANC-1 viability (**Figure 4.15, 4.18**). Cell viability was evaluated in hydrogels fabricated using 5 and 20 kDa PEG4eNB macromers and initial viability post-encapsulation was measured as described previously. Qualitative Live/Dead staining results indicated a reduction in viability from ~90% to ~77% with decrease in PEG4eNB M.W. regardless of the linker used (**Figure 4.17**). As explained previously in **Section 4.1.2**, that decreasing PEG4eNB M.W. from 20 kDa to 5 kDa resulted in higher hydrogel shear modulus i.e., ~3.1 and ~5.5 kPa for 20 kDa and 5 kDa PEG4eNB respectively at the same polymer concentration (**Figure 4.3**). The drastic increase in modulus due to decreasing macromer M.W. resulted in higher network crosslinking [70], causing higher degree of environmental stresses which, negatively affect initial PANC-1 cell survival.

4.3.2 Influence of Crosslinker Type on Long-Term PANC-1 Growth and Activity

Depending on the cross-linker chemistry, thiol-ene hydrogels can be manipulated to undergo hydrolysis or proteolysis at varying degrees (**Table 3.1**). For example, when crosslinked with DTT (a non-enzyme sensitive linker), thiol-ene hydrogels undergo slow hydrolytic degradation compared to bis-cysteine peptide cross-linkers. When crosslinked with CGGYC [27] or MMP_{scrm} (a non-MMP sensitive linker) [89], thiol-ene hydrogels only endure fast hydrolytic degradation compared to MMP_{Linker} (MMPs sensitive linker) [90, 91] where the hydrogels not only experience fast hydrolytic degradation but are also susceptible to MMP proteolysis. We hypothesized that cross-linker type and sensitivity directly affects cellular morphogenesis in 3D thiol-ene hydrogels. Here, we first visualized PANC-1 morphogenesis in 5 wt.% PEG4NB hydrogels over a course of 10 days using Live/Dead staining followed by confocal imaging at day 4, 7 and 10 (**Figure 4.16a**). As shown in **Figure 4.16a**, PANC-1 cell proliferate in thiol-ene hydrogels regardless of the linker used but the rate of proliferation and cell morphogenesis depends on linker chemistry. For example, PANC-1 cells proliferate faster in hydrogels crosslinked with MMP_{Linker} over a period of 14 days and form cyst-like clusters compared to cells in both CGGYC and MMP_{scrm} crosslinked hydrogels, where PANC-1 cells show slower proliferation rate and form compact and rounded clusters.

Previously, it has been shown that PANC-1 cells in response to environmental stresses such as matrix stiffness, secrete MMPs allowing cells to degrade the surrounding ECM to relieve unfavorable stresses [105-110]. Since all bis-cysteine peptide linkers used for thiol-ene crosslinking undergo similar rate of hydrogel hydrolytic degradation (**Figure 4.2**), the observe difference in PANC-1 cell morphogenesis may be attributed to the varying sensitivity of linkers to cell mediated proteolysis. We hypothesize that MMP_{Linker} crosslinked hydrogels due to its sensitivity to cell secreted MMPs allow encapsulated PANC-1 cells to remodel their microenvironment and proliferate at a higher rate due to coupled effect of both hydrolytic and enzymatic degradation. On the other hand, proliferation of PANC-1 cells when encapsulated in non-MMP sensitive hydrogels depends on hydrolytic degradation due to no protease sensitivity.

As discussed previously, PANC-1 cells cultured in 3D pancreatic epithelium like environment form cysts, a characteristic feature of ductal epithelial cells [72, 111, 112]. Similar to previous work, PANC-1 cells in MMP$_{Linker}$ crosslinked hydrogels exhibit their cyst-like phenotype due to cell matrix remodeling. Compared to cyst formation in MMP sensitive hydrogels, we speculate that PANC-1 cells in non-MMP sensitive hydrogels mainly form compact clusters due to the inability of cells to remodel its ECM and cell reliance on hydrogel hydrolytic degradation to relieve matrix induced environmental stresses.
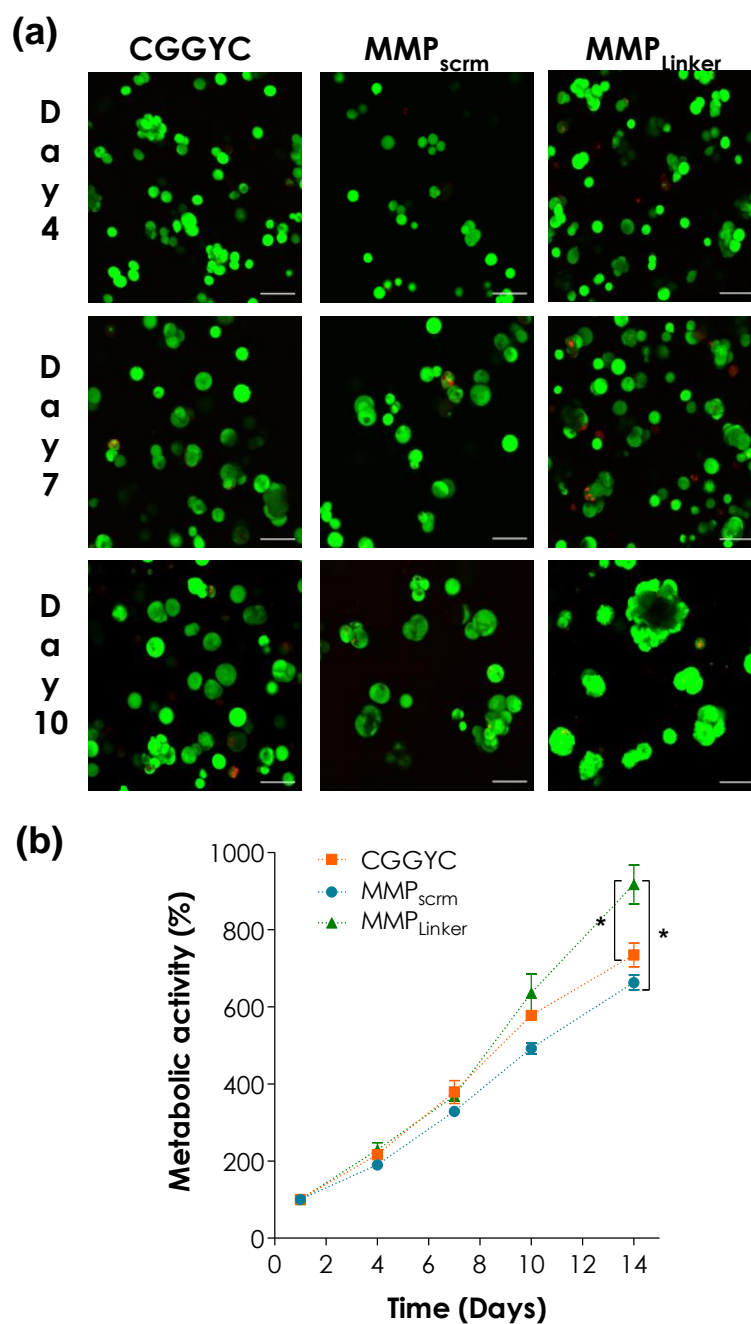
Figure 4.16. Effect of cross-linker chemistry on PANC-1 cell morphogenesis (PEGe4NB: 20 kDa, 5 wt%) (a) PANC-1 cell morphology visualized using Live/Dead staining and confocal microscopy (z-stack images) at day 4, 7, and 10 (Scales: 100µm). (b) Cell metabolic activity measured as a function of time by AlamarBlue® reagent. All readings were normalized to day-1 values in respective group (N = 4, mean ± S.D.). Asterisk represent $p < 0.05$ between indicated group.

Next, we assessed the effect of linker type on long-term PANC-1 cell survival quantitatively using AlamarBlue® reagent. We obtained PANC-1 relative metabolic activity by normalizing the reagent fluorescence signal to that acquired at day 1 (**Figure 4.16b**). Similar to results obtained via Live/Dead staining, we found that PANC-1cells are metabolically active in all hydrogel formulations and the cellular activity increases over the period of 14 days indicating cell proliferation. Comparing linker types i.e. CGGYC, MMP_{scrm} and MMP_{Linker}, we observe slight difference between relative metabolic activity profiles until day 10. But at day 14, cells encapsulated in MMP_{Linker} crosslinked hydrogels show significantly higher metabolic activity compared to cells in CGGYC or MMP_{scrm} crosslinked hydrogels. Studies have shown that the process of cyst formation involves three main steps: (1) compact cluster formation due to proliferation or migration, (2) cell death in the core due to hypoxia induced by peripheral cells, and (3) further peripheral cell proliferation [111]. Some studies have argued that step 3 happens first followed by cell death and a few argue that 2 and 3 happen at the same time, but in essence the process of cyst formation remains the same throughout literature [72, 112]. With the knowledge that PANC-1 cells in MMP_{Linker} crosslinked hydrogels proliferate and remodel their matrix and the end result is cyst-like cluster formation, we can hypothesize that the similarity in metabolic activity profile of cells in MMP_{Linker} and CGGYC or MMP_{scrm} crosslinked hydrogels at day 10 is due to cell death during the process of cyst formation in PEG4eNB/MMP_{Linker} hydrogels. And the increase in cell metabolic activity at day 14 in PEG4eNB/MMP_{Linker} was due to the outward proliferation of the peripheral cells of the cyst. Further studies are required to test the afore mentioned hypothesis.

(a)

(b)
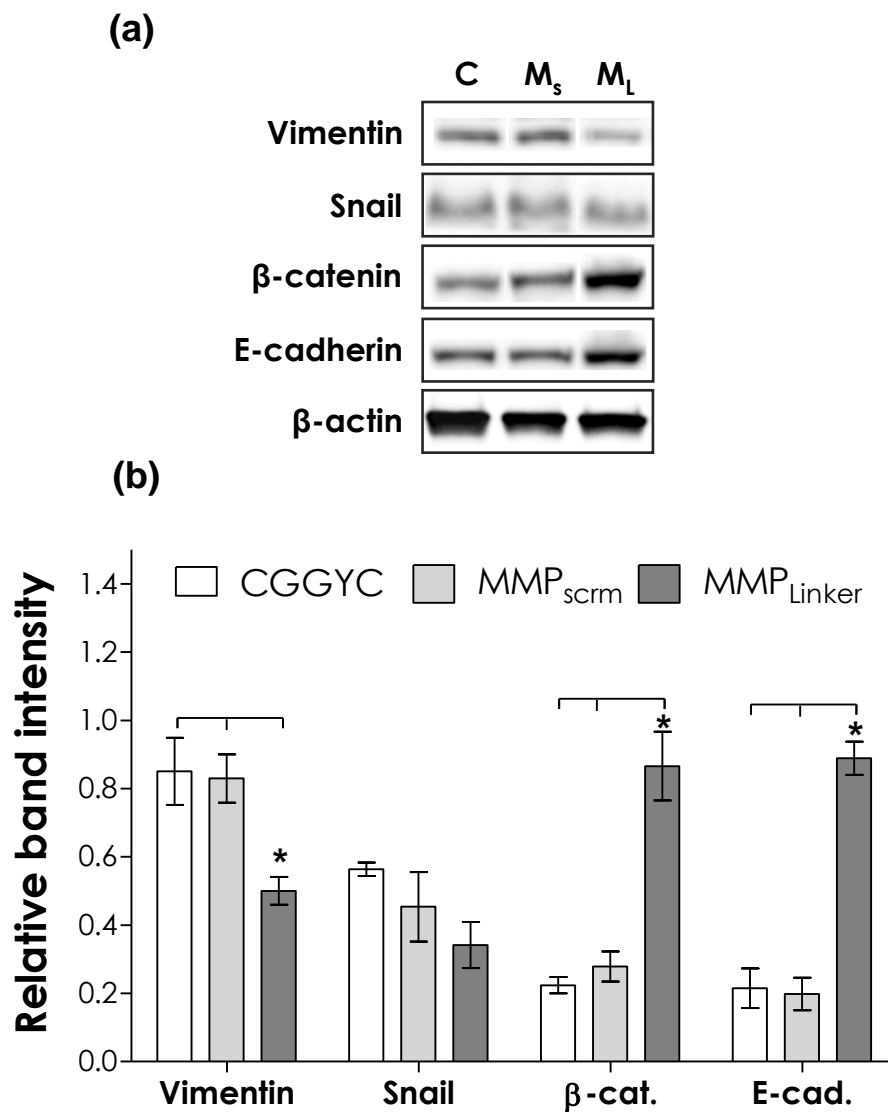
Figure 4.17. Effect of cross-linker chemistry on PANC-1 cell morphogenesis at protein level. (a) Western blotting analysis for mesenchymal (Vimentin, Snail) and epithelial (β-catenin and E-cadherin) lineage specific markers 10 days post-encapsulation (C: CGGYC, M_s: MMP$_{scrm}$, M_L: MMP$_{Linker}$). (b) Semi-quantitative analysis of protein band intensities. All band intensities were obtained by ImageJ and normalized to the band intensity of β-actin in respective group (N = 4, mean ± S.D.). Asterisk represent $p < 0.05$ between indicated group.

Previous studies performed on kidney, lung and breast carcinoma cells in 2D have shown that all these epithelium derived cells are capable of undergoing both epithelial to mesenchymal transition (EMT) when subjected to stressful conditions and mesenchymal to epithelial transition (MET) when conditions are restored back to match the epithelioid cell microenvironment [113, 114]. With this information and observed cell morphogenesis in mind, we evaluated PANC-1 cell morphogenesis by measuring cell protein expression of key epithelial markers (β-catenin, E-cadherin) and mesenchymal markers (Vimentin and Snail) [114] using western blotting and band analysis techniques 10 days after culture in 5 wt.% PEG4eNB hydrogels (**Figure 4.17**).

We found that PANC-1 cells in both PEG4eNB/CGGYC and PEG4eNB/MMP$_{scrm}$ hydrogels express significantly higher levels of Vimentin and significantly lower levels of β-catenin and E-cadherin. In contrary, cell in PEG4eNB/MMP$_{Linker}$ hydrogels show higher levels of β-catenin and E-cadherin; and lower levels of Vimentin compared to other experimental groups. Previous studies have indicated that epithelial cells including PANC-1 cells when cultured on 2D surface express high levels of epithelial markers such as cytokeratin, β-catenin, E-cadherin, Claudins and others, and little to no expression of mesenchymal markers such as Vimentin, Snail, Slug, N-cadherin and others [72, 73]. Comparing information from previous findings, results obtained in our study indicate that PANC-1 cell in 3D thiol-ene hydrogels regardless of the crosslinker chemistry, experience stress due to network crosslinking and as a consequence express Vimentin and Snail1 (EMT markers). PANC-1 cells in PEG4eNB hydrogels with no protease sensitive linker (such as CGGYC or MMP$_{scrm}$), remain in stressed state due to network restriction and maintain high expression of the above mentioned EMT markers.

On the other hand, cells encapsulated in protease sensitive hydrogels remodel their matrix, opening up the hydrogel network to allow for cell proliferation and cyst formation, resulting in high levels of β-catenin and E-cadherin (epithelial markers) and relatively lower levels of EMT markers. These western blotting results (**Figure 4.17**) correlate well with the cell viability results acquired using Live/Dead staining and

AlamarBlue® assay (**Figure 4.16**), and provides further insight into the effects of changing matrix conditions on PANC-1 cell behavior at protein level.

4.3.3   Effect of Gel Stiffness and Degradability on PANC-1 Morphogenesis

Several studies have reported that stiffness of hydrogels plays a significant role in regulating phenotypes of various cells types [38, 115-117] including epithelial cells, i.e. matrix rigidity modulates whether a cell will undergo EMT or not [118]. To study the effect of matrix stiffness on PANC-1 cellular morphogenesis and metastasis, we encapsulated PANC-1 cells at a cell packing density of 2 ẋ 10^6 cells/mL in 5 wt.% 5 and 20 kDa PEG4eNB hydrogels crosslinked by either DTT or MMP$_{Linker}$. Cell morphogenesis was observed using Live/Dead staining, cell viability as a function of time was measured using AlamarBlue® reagent**,** and finally PANC-1 protein expressions were assessed using western blotting (**Figure 4.19, 4.20**).

As shown in **Figure 4.19** cells survive in both higher and lower stiffness but with varying degree of cell proliferation. We found that more cells die over a period of 10 days in lower M.W. (5 kDa) PEG4eNB/DTT hydrogels compared to cells encapsulated in 20 kDa PEG4eNB/DTT hydrogels. Further, we observed that PANC-1 cells in 5 kDa MMP sensitive hydrogels show protrusion (like mesenchymal cells) compared to cyst formation in 20 kDa protease sensitive PEG4eNB hydrogels (**Figure 4.19a, 4.19b**). In addition to differences in cellular morphology, PANC-1 cells present significantly higher metabolic activity with time in MMP sensitive hydrogels regardless of PEG4eNB molecular weight, while cells in non-protease sensitive DTT crosslinked show a steady activity profile over time (**Figure 4.19c, 4.19d**). At protein level, PANC-1 cells in 20 kDa MMP$_{Linker}$ crosslinked PEG4eNB hydrogels express significantly higher levels of epithelial markers (β-catenin and E-cadherin) and lower level of mesenchymal markers (Vimentin and Snail1) compared to all other experimental groups (**Figure 4.20**).
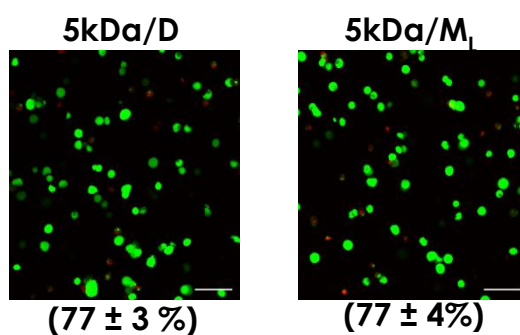
Figure 4.18. Effect of PEG4eNB molecular weight on initial PANC-1 viability measured using Live/Dead staining kit (D: DTT; M_L: MMP_{Linker}). Numbers shown below the representative confocal z-stack images are the percentage of live cells over total cell count (Scale: 100μm; N = 4, mean ± S.D.).
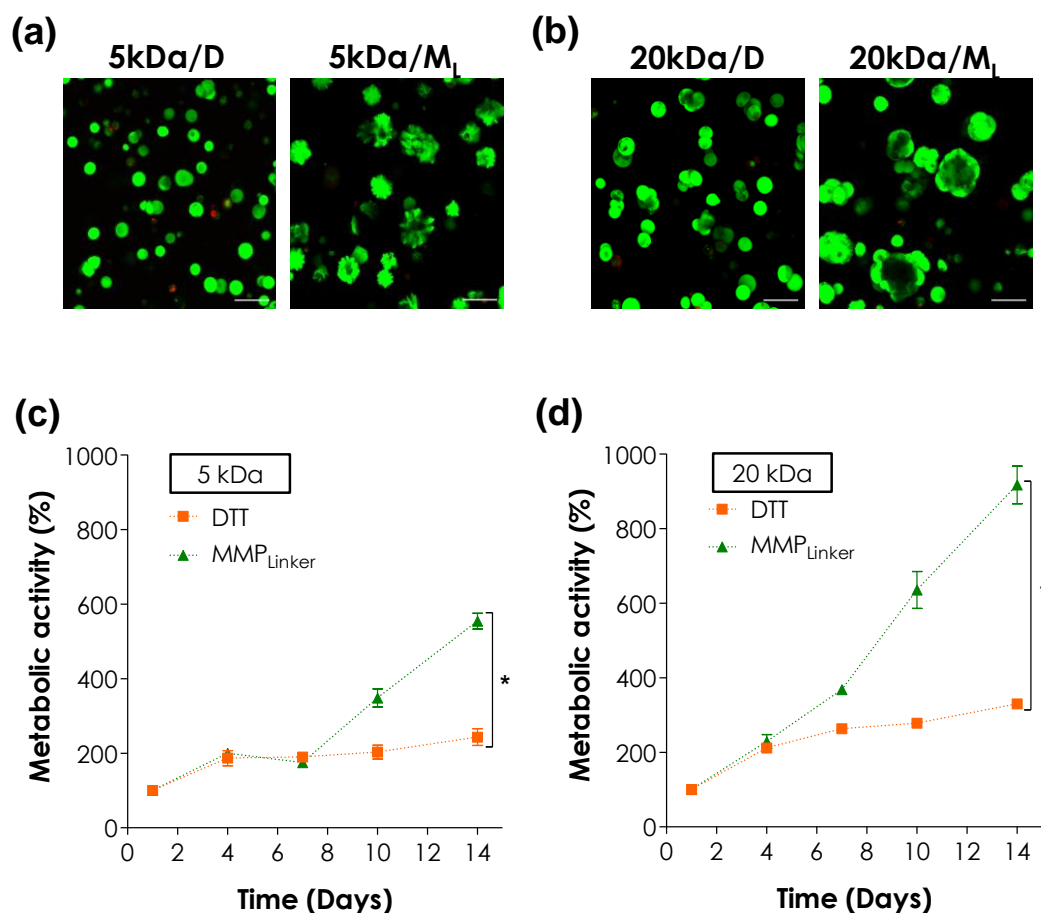
Figure 4.19. Effect of PEG4NB molecular weight and cross-linker chemistry on PANC-1 cell morphogenesis (PEG4eNB: 5wt%). (a-b) Representative confocal z-stack images of PANC-1 cell morphology (Live/Dead stain 10 days post-encapsulation) in gels formed by different PEG4eNB molecular weights (a: 5kDa; b: 20kDa) and cross-linker chemistries (D: DTT; M_L: MMP_{Linker}) (Scales: 100µm). (c-d) Cell metabolic activity measured by AlamarBlue® reagent and normalized to day-1 value in the respective group. (c: 5kDa; d: 20kDa PEG4eNB). (N = 4, mean ± S.D.) Asterisk represent $p < 0.05$ between indicated group.

As mentioned previously, PANC-1 cells like other epithelial cells undergo epithelial to mesenchymal transition (EMT) in unfavorable or extremely stressful conditions [113, 114]. Hydrogels fabricated using lower M.W. PEG4eNB exhibit higher shear modulus compared to higher M.W. PEG4eNB hydrogels (**Figure 4.3**), due to formation of tighter network with smaller mesh size. Previous studies have shown that stress induced by matrix stiffness creates a hostile environment for cells and triggers EMT allowing cells to escape unfavorable matrix conditions [118]. The observed protrusion and higher levels of mesenchymal markers in 5 kDa PEG4eNB/MMP$_{Linker}$ hydrogels are due to the PANC-1 cell struggle to free itself from the rigid microenvironment. Live/Dead images of cells in 5 kDa DTT crosslinked hydrogels do not show protrusion due to the insensitivity of hydrogel to MMP secretion but the stress induced by the matrix can be clearly seen through protein analysis revealing higher levels of Vimentin and Snail1. These results suggest that PANC-1 cells could be held in mesenchymal state if stressful conditions are maintained over time. On the other hand, epithelial phenotype can be restored if cells are allowed to remodel the surrounding ECM and relieve the induced stresses.
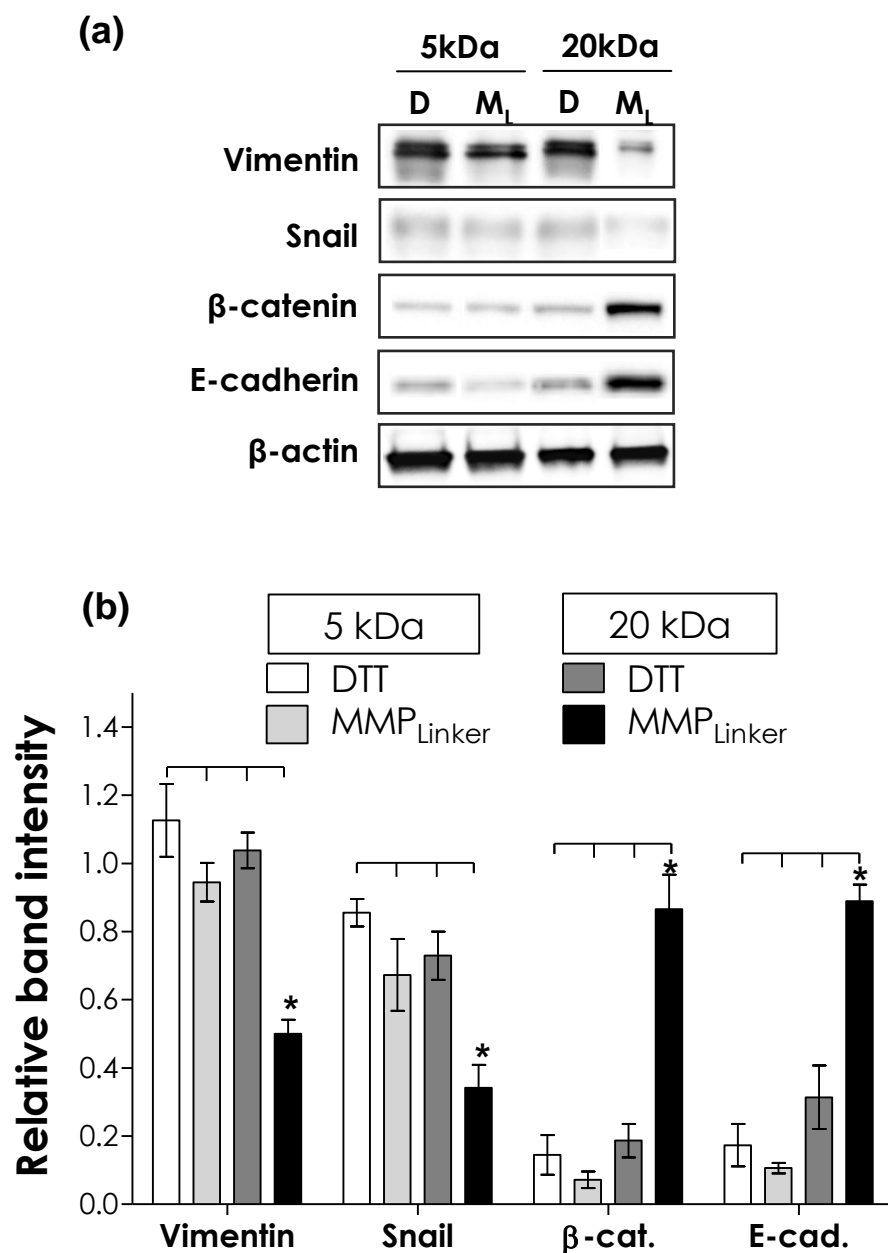
Figure 4.20. Effect of PEG4NB molecular weight and cross-linker chemistry on PANC-1 cell morphogenesis at protein level. (a) Western blotting analysis for mesenchymal (Vimentin, Snail) and epithelial (β-catenin and E-cadherin) lineage specific markers 10 days post-encapsulation (D: DTT, M_L: MMP_{Linker}). (b) Semi-quantitative analysis of protein band intensities. All band intensities were obtained by ImageJ and normalized to the band intensity of β-actin in respective group (N = 4, mean ± S.D.). Asterisk represent $p < 0.05$ between indicated group.

4.3.4   Cell Morphology in Blank Slate Hydrogels

As discussed previously, PANC-1 cells form cyst like structures in suitable 3D microenvironment [72, 111, 112]. But in contrary to the above observation, PANC-1 cells in 3D thiol-ene hydrogels exhibit varying morphologies as shown in **Figure 4.16a, 4.19a, 4.19b, 4.21**. After a complete screening of Live/Dead images five major morphologies were observed, namely: (I) Single cell, (II) Small rounded and compact cell clusters, (III) Large and irregular cell clusters, (IV) Small clusters with short cellular protrusions and (V) Cyst-like cell clusters. After morphology categorization, immunostaining was utilized to visualize the pattern of f-actin (structural protein) and β-catenin (cell-ECM and cell-cell interaction protein) [114] (**Figure 4.21**).

We observed that single cell (I) showed f-actin and β-catenin staining around the nuclei indicating cytosolic location of these proteins. Similar protein staining pattern were observed in small and rounded compact cell clusters (II) i.e. compact and evenly distributed f-actin and β-catenin staining. In contrary, larger and irregular cell clusters (III) showed irregular f-actin and β-catenin staining around the cluster with some regions with more concentrated protein staining than the other regions. For cell cluster with short cellular protrusions (IV) f-actin staining was consistent with the direction of cell protrusion and minimal to no β-catenin staining was observed. Lastly, cyst-like clusters (V) exhibited concentrated f-actin and β-catenin staining in the hollow core of the aggregate and regular staining levels in the peripheral region of the clusters. Studies performed on epithelial cyst in 3D have shown that cells concentrate ECM based proteins in the hollow core in order to support the cyst architecture and allow for peripheral growth in non-interactive matrix [112]. The results obtained are consistent with previous studies which present cyst with similar protein staining patterns and feature (using Live/Dead staining dead cells marked by red stain were observed in the core of the cyst (**Figure 4.16a, 4.19a**)).

DAPI/β-catenin/F-actin
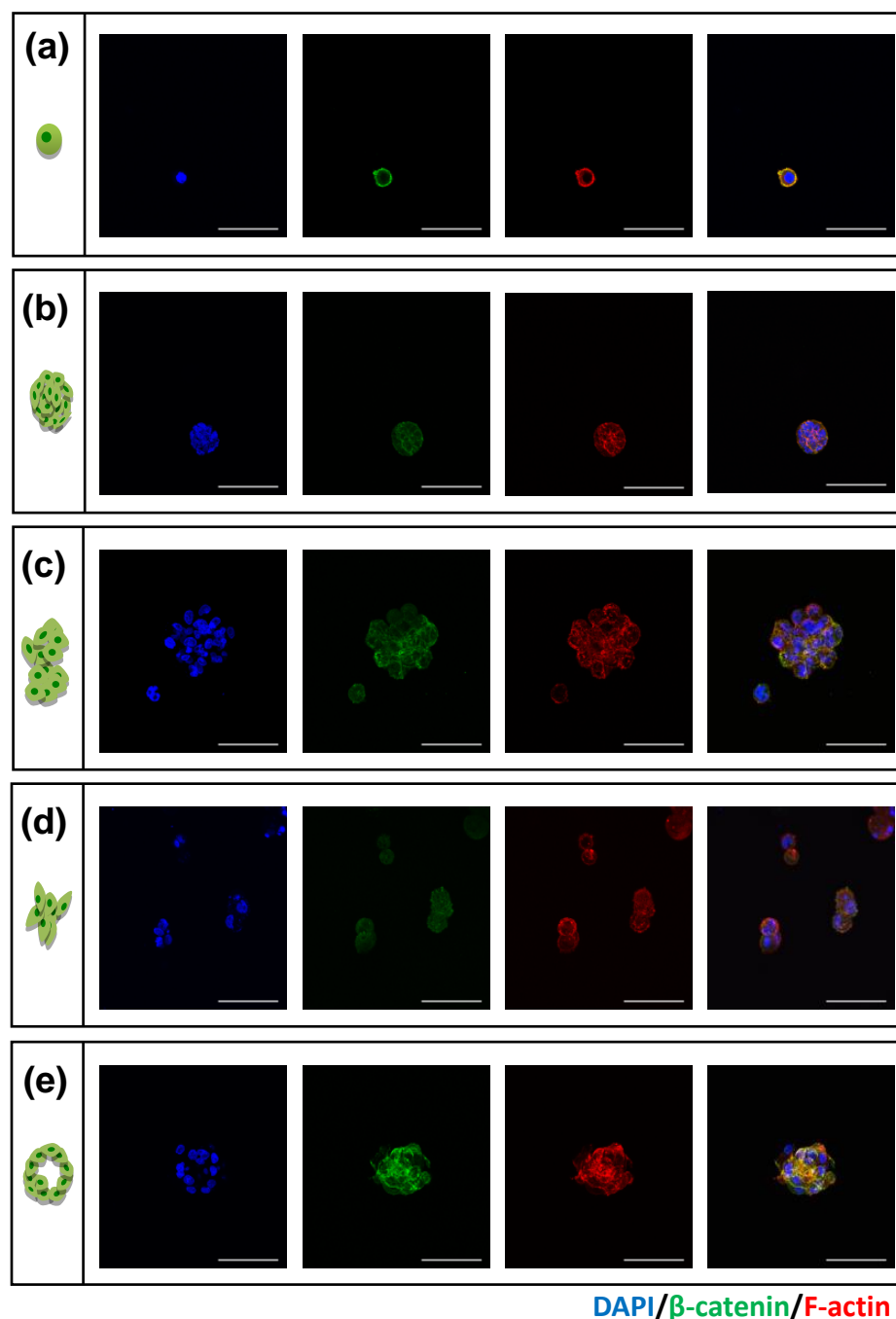
Figure 4.21. Representative immunostaining images of PANC-1 cells encapsulated in PEG4eNB hydrogels. At day 10 post-encapsulation, PANC-1 cells were stained using antibodies targeting β-catenin (green) and F-actin (red). Cell nuclei were counter-stained with DAPI (blue). (a) Single cell; (b) Small rounded and compact clusters; (c) Large and irregular cell clusters; (d) Small clusters with short cellular protrusions; and (e) Cyst-like cell clusters. (Scales: 100µm)

After establishing the features commonly exhibited by each PANC-1 cluster, Live/Dead images acquired at day 10 were analyzed to assess the effect of macromer composition on total population of each morphology category (**Figure 4.24a**). We found that when PANC-1 cells were encapsulated in DTT crosslinked hydrogels regardless of the PEG4eNB M.W., major cell population exhibit, single cells (I) and round and compact cell clusters (II) with minimal to no cyst formation. Further, major cell population in 5 kDa PEG4eNB/MMP$_{Linker}$ hydrogels had small clusters with short cellular protrusions (IV). When cells were encapsulated in MMP$_{Linker}$ crosslinked 20 kDa PEG4eNB hydrogels, higher number of hollow cyst like clusters (V) and large and irregular cell clusters (III) were observed compared to all other test groups.

In addition to morphology analysis, we also measured the size of encapsulated PANC-1 clusters from the Live/Dead staining images obtained 10 days post-encapsulation (**Figure 4.25a**). We found that increasing matrix stiffness resulted in decreased cluster size, more specifically MMP$_{Linker}$ crosslinked 20 kDa PEG4eNB hydrogels supported formation of larger PANC-1 clusters ~74 μm in size compared to ~56 μm clusters in 5 kDa PEG4eNB hydrogels. These PANC-1 morphology and size results in 3D thiol-ene hydrogels suggest that varying macromer composition provide not only intrinsic protein level control but also extrinsic phenotypic control.

4.3.5 Influence of ECM Motifs on PANC-1 Cell Morphogenesis

It should be noted that results shown in **Figures 4.16** through **4.21** were obtained from PEG4eNB hydrogels without the presence of any bioactive moieties, which have proven beneficial in supporting cell survival in 3D on multiple occasions [93, 112, 119-121]. To evaluate the effect of bioactive motifs on PANC-1 cell survival and morphogenesis, we monitored PANC-1 cell behavior in 5wt% CGGYC cross-linked PEG4eNB hydrogels immobilized with 0, 1, and 2 mM of CRGDS (fibronectin derived) and KCYIGSR (laminin derived) using Live/Dead staining, AlamarBlue® reagent and western blotting (**Figure 4.22, 4.23**). The incorporation of RGDS motif in non-MMP

sensitive hydrogels resulted in a higher degree of (1) PANC-1 metabolic activity (**Figure 4.22c**) and (2) greater cyst formation (**Figure 4.22a**), while the addition of YIGSR had no effect of on cellular activity (**Figure 4.25d**) but more dead cells and highly compact clusters were observed (**Figure 4.25b**) compared to both RGD containing hydrogel and hydrogels with no bioactive moieties. Protein analysis revealed no significant difference in the levels of Vimentin and Snail1 across all test groups. On the other hand, cells in hydrogels conjugated with both 1 and 2 mM of YIGSR compared to non-bioactive and RGD containing hydrogels endured higher levels of β-catenin and E-cadherin (**Figure 4.23**).
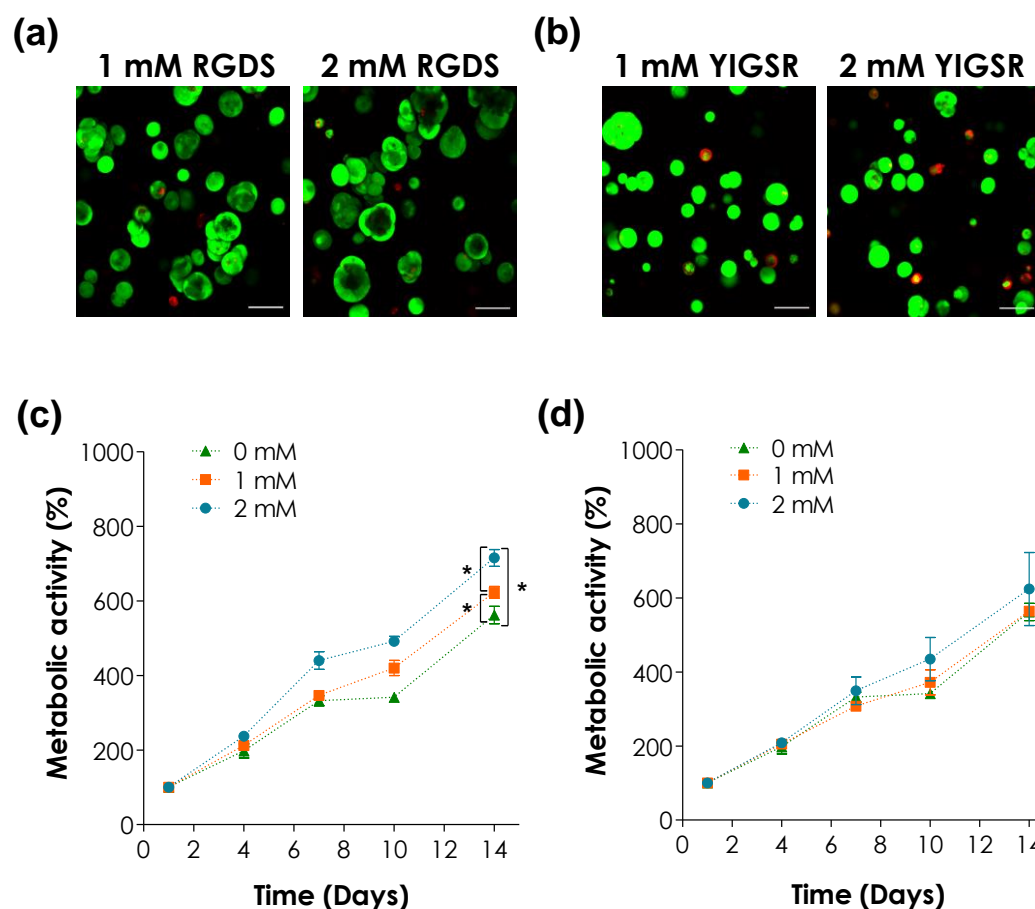
Figure 4.22. Effect of ECM-mimetic motifs on PANC-1 cell morphogenesis (PEG4eNB: 20kDa, 5wt%). (a-b) Representative confocal z-stack images of PANC-1 cell morphology (Live/Dead stain 10 days post-encapsulation) in gels immobilized with different ECM-mimetic motifs (a: CRGDS; b: KCYIGSR) (Scales: 100μm). (c-d) Cell metabolic activity measured by AlamarBlue® reagent and normalized to day-1 value in the respective group (c: CRGDS; d: KCYIGSR). (N = 4, mean ± S.D.) Asterisk represent $p < 0.05$ between indicated group.

Previous studies have shown that RGDS (a fibronectin based adhesive) ligand provides adhesion sites for cells and enhances cell morphogenesis, while YIGSR (a Laminin based) ligand assists in cell aggregation [121]. The results obtained in this study agree with previous finding i.e. PANC-1 cells in the presence of RGDS motif are more bioactive and due to matrix interaction express their ductal epithelial phenotype by forming more cyst like clusters [112, 121]. On the other hand, PANC-1 cells in the presence of YIGSR motif are forced to aggregate and form more rounded and compact clusters [121]. Further, cells in all gel formulations experience matrix based stresses as indicated by the presence of mesenchymal markers but the ECM support provided by RGDS allows cells to proliferate to a higher degree and exhibit their epithelial like phenotype. YIGSR conversely, forces cell to aggregate into clusters but does not allow them to exhibit ductal epithelial phenotype by restricting cyst formation via intracellular stress induction, pushing cells to interact with themselves to survive. This level of cellular morphogenesis control via matrix manipulation can further allow us to push PANC-1 cells towards endocrine differentiation in 3D.
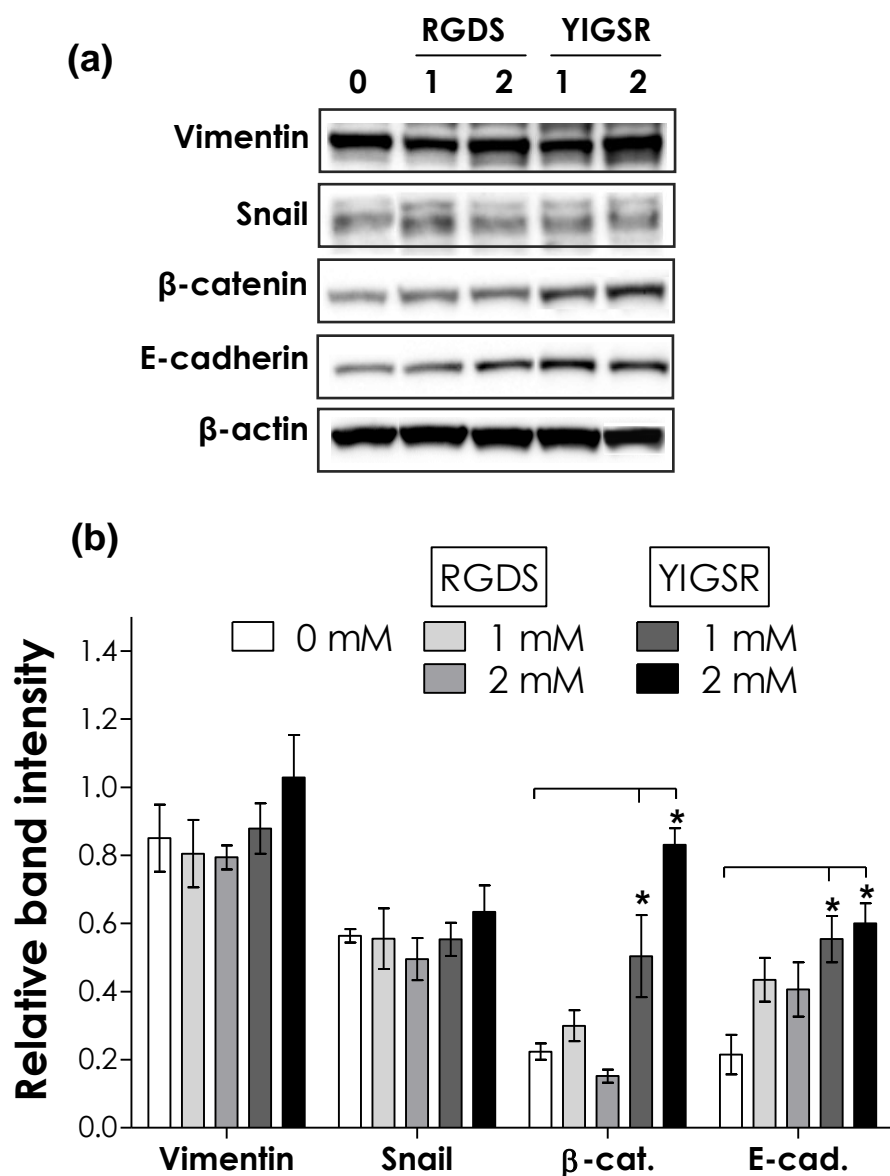
Figure 4.23. Effect of ECM-mimetic motifs on PANC-1 cell morphogenesis at protein level. (a) Western blotting analysis for mesenchymal (Vimentin, Snail) and epithelial (β-catenin and E-cadherin) lineage specific markers 10 days post-encapsulation in gels immobilized with different ECM-mimetic motifs (CRGDS; KCYIGSR). (b) Semi-quantitative analysis of protein band intensities. All band intensities were obtained by ImageJ and normalized to the band intensity of β-actin in respective group (N = 4, mean ± S.D.). Asterisk represent $p < 0.05$ between indicated group.

4.3.6   Cell Morphology in Bioactive Hydrogels

In addition to cell viability and protein expression, the effects of ECM motifs on total population of each morphology category and cluster size were evaluated using previously described method (**Figure 4.24b, 4.25b**). We observed that the number of large and irregular cell clusters (III) and cyst like clusters (V) significantly increased with increasing concentration of immobilized RGDS in PEG4eNB/CGGYC hydrogels compared to hydrogels with 0 mM of RGDS which contains more single cells (I) and small rounded and compact cell clusters (II). In contrary to RGDS, increasing YIGSR concentration resulted in a slight increased number of small rounded and compact clusters (II) but the increase was not found significant when compared to cells in non-bioactive PEG4eNB/CGCYC hydrogels.
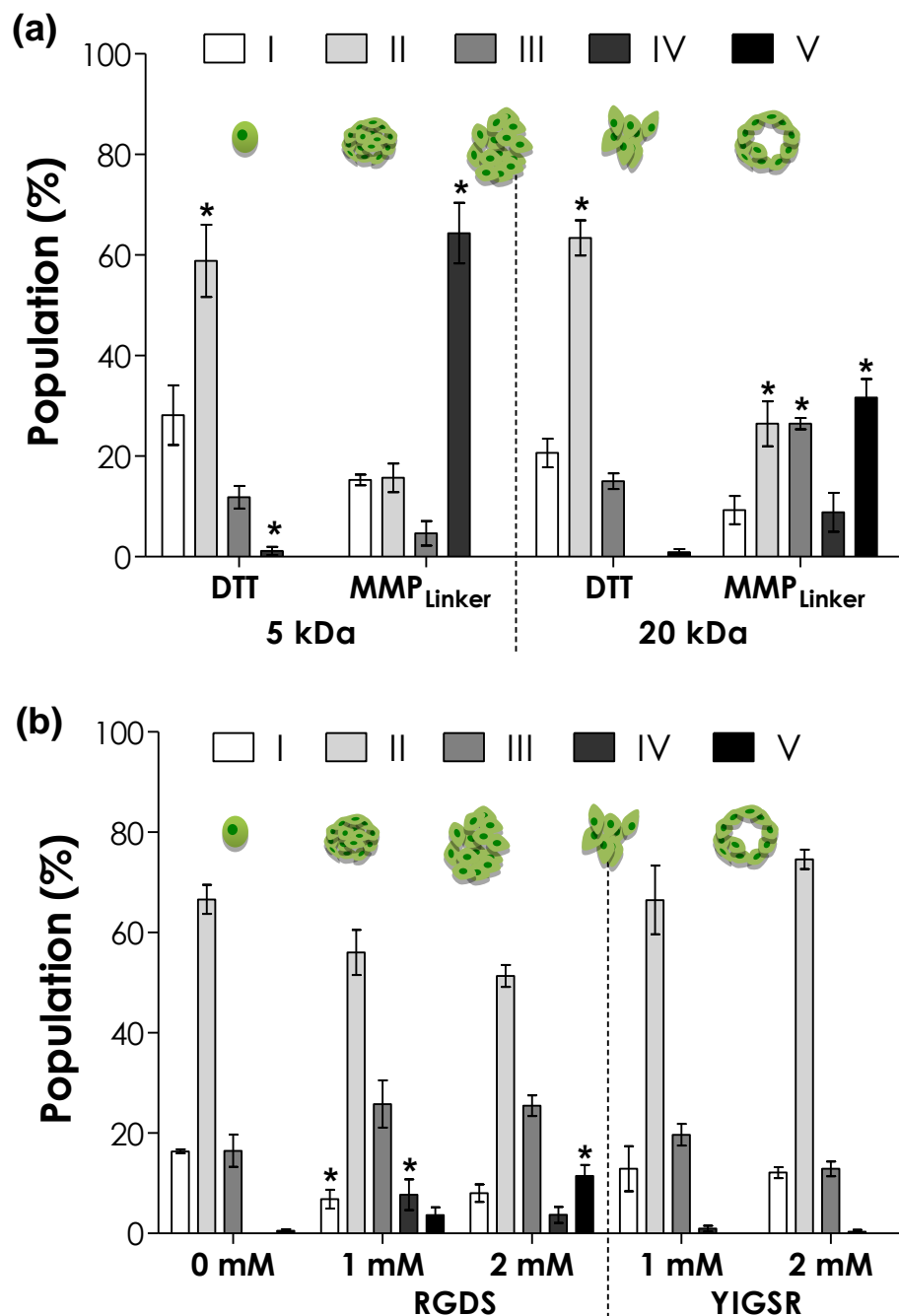
Figure 4.24. Categorization of PANC-1 cell morphology in PEG4eNB (at 5wt%) hydrogels with: (a) varying molecular weight and cross-linker chemistry; and (b) varying ECM-mimetic motifs. Live/Dead staining images were used to analyze cell morphology at day-10 post-encapsulation (N = 4, mean ± S.D.). Category I in each gel formulation was utilized to perform statistical analysis in (a). 0 mM ligand concentration group in each category was utilized for statistical analysis in (b). Asterisk represent p < 0.05.

Additionally, cluster size can also be controlled by incorporating bioactive motifs, for example addition of RGD resulted in a significant increase in PANC-1 aggregate diameter from 58.5 ± 2.9 μm to 71.6 ± 2.3 μm. In contrary, addition of YIGSR reduces PANC-1 cell cluster from 58.5 ± 2.9 μm to 52.3 ± 1.1 μm. These morphology and size results suggest that in addition to controlling intrinsic cell behavior, cellular morphogenesis can also be controlled via step by step matrix manipulation.
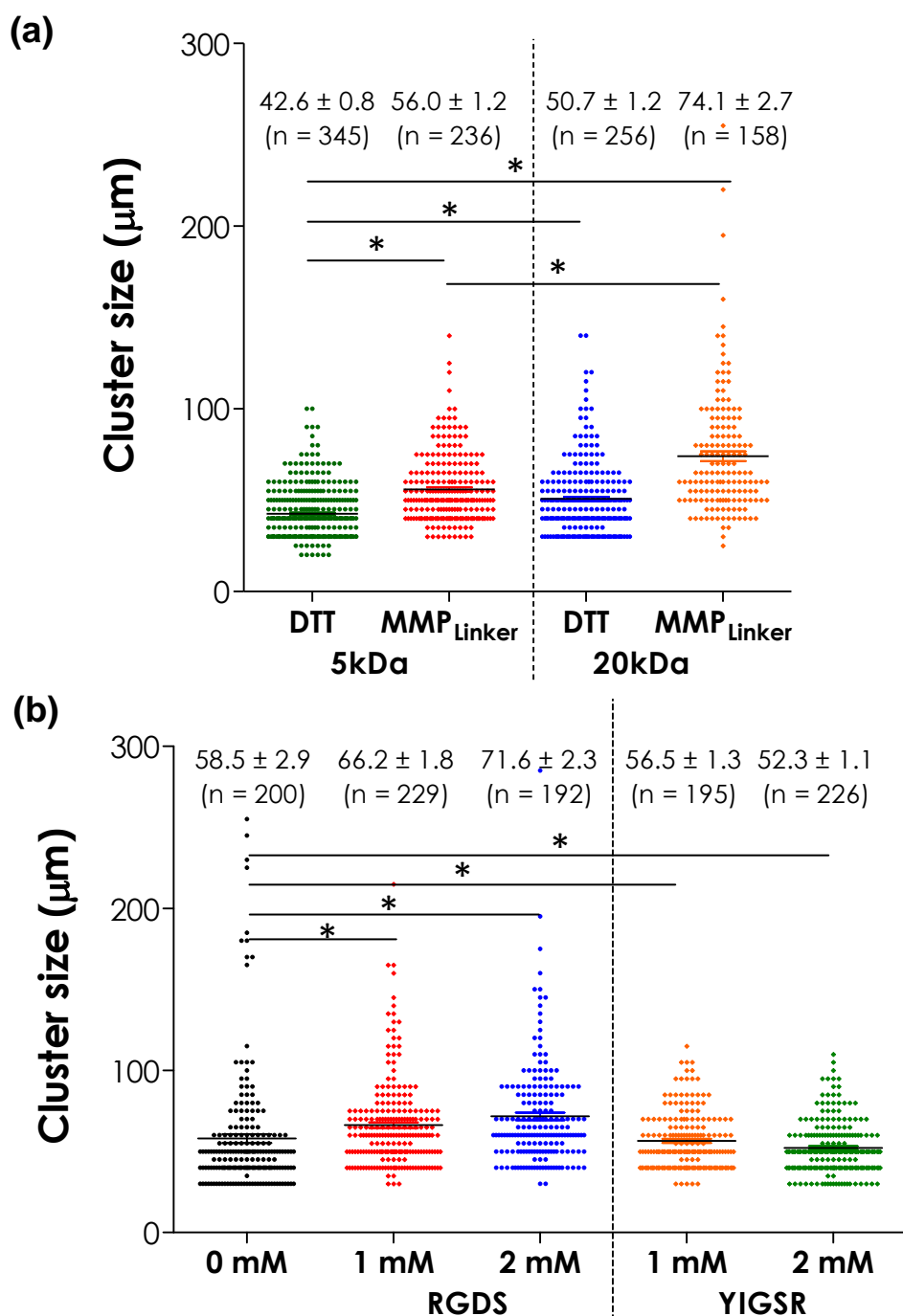
Figure 4.25. Influence of hydrogel formulation on distribution of PANC-1 cell cluster size in PEGe4NB (at 5wt%) with: (a) varying molecular weight and cross-linker chemistry; (b) varying ECM-mimetic motifs. Live/Dead staining images were used to analyze cell cluster size at day-10 post-encapsulation (N = 4, mean ± S.D.). Asterisk represent $p < 0.05$ between indicated groups.

5. CONCLUSION AND FUTURE DIRECTIONS

In summary, this study has shown that thiol-norbornene hydrogels could be designed to remain stable, or be tuned to degrade hydrolytically and/or proteolytically. Further, hydrogel can be conjugated with ligands to enhance the bioactivity of thiol-ene hydrogels. Overall, thiol-ene hydrogels provided a cytocompatible environment for promoting MIN6 β-cell, hMSC and PANC-1 cell survival, proliferation, and morphogenesis in 3D. In addition, cell viability, proliferation, and morphology were affected greatly by hydrogel formulations, degradability, and bioactivity. Lower macromer contents reduced initial cell damage during *in situ* photo-encapsulation due to lower radical concentration, lower degree of cross-linking reaction, and decreased network cross-linking density. More importantly, hydrolytic degradation, proteolytic matrix remodeling, and cell-matrix interaction exhibited synergistic effect on promoting cell survival, proliferation, and morphogenesis (e.g., larger cell spheroids in MIN6 β-cells, higher degree of cell spreading in hMSCs and increased PANC-1 cyst formation). Due to the highly versatile nature of thiol-ene hydrogels, we were able to identify the conditions that favored both epithelial and/or mesenchymal morphogenesis for all cell types studied.

The results obtained after evaluating various factors both at matrix and cellular level that affect epithelial and/or mesenchymal morphogenesis in 3D, indicate that cell morphogenesis in 3D can be controlled by simple thiol-ene network manipulation. In this study we have established hydrogel formulations that can be: (1) utilized for long-term preservation of sensitive cells such pancreatic β-cells and islets: (2) used to study cancer metastasis in 3D using various carcinoma cells; and (3) exploited to differentiate exocrine

pancreatic cells such as PANC-1 cells towards endocrine function to support cell-based therapy for treating type I diabetes.

In future, the information obtained from this study will be utilized to (1) design better immunoisolation barriers for islets using thiol-ene chemistry; (2) study and control pancreatic cancer metastasis in 3D thiol-ene hydrogels using PANC-1 cells, COLO-357 cells, ASPC-1 cells and other pancreatic carcinoma cell lines; (3) differentiate PANC-1 cells (exocrine cells) to islet like clusters (ILCs) (endocrine cells) to provide abundant cell supply for islet transplantation. Both study directions will help support therapeutics towards pancreatic diseases namely: pancreatic cancer and type I diabetes which affects millions of people worldwide.

LIST OF REFERENCES

LIST OF REFERENCES

[1]   R. Jain and E. Lammert, "Cell-cell interactions in the endocrine pancreas," *Diabetes Obes Metab,* vol. 11 Suppl 4, pp. 159-67, Nov 2009.

[2]   R. N. Kulkarni, "The islet beta-cell," *Int J Biochem Cell Biol,* vol. 36, pp. 365-71, Mar 2004.

[3]   R. C. Vasavada, J. A. Gonzalez-Pertusa, Y. Fujinaka, N. Fiaschi-Taesch, I. Cozar-Castellano, and A. Garcia-Ocana, "Growth factors and beta cell replication," *Int J Biochem Cell Biol,* vol. 38, pp. 931-50, 2006.

[4]   M. Virreira, J. Perret, and C. Delporte, "Pancreatic beta-cells: Role of glycerol and aquaglyceroporin 7," *Int J Biochem Cell Biol,* vol. 43, pp. 10-3, Jan 2011.

[5]   H. S. Kim and M. S. Lee, "Role of innate immunity in triggering and tuning of autoimmune diabetes," *Curr Mol Med,* vol. 9, pp. 30-44, Feb 2009.

[6]   J. Diana, L. Gahzarian, Y. Simoni, and A. Lehuen, "Innate immunity in type 1 diabetes," *Discov Med,* vol. 11, pp. 513-20, Jun 2011.

[7]   C. G. Fanelli, F. Porcellati, S. Pampanelli, and G. B. Bolli, "Insulin therapy and hypoglycaemia: the size of the problem," *Diabetes Metab Res Rev,* vol. 20 Suppl 2, pp. S32-42, Nov-Dec 2004.

[8]   J. E. Candiello, M. Jaramillo, S. K. Goh, and I. Banerjee, "Role of substrates in diabetes therapy: stem cell differentiation and islet transplantation," *Crit Rev Biomed Eng,* vol. 39, pp. 535-55, 2011.

[9]   A. M. Shapiro, J. R. Lakey, E. A. Ryan, G. S. Korbutt, E. Toth, G. L. Warnock, N. M. Kneteman, and R. V. Rajotte, "Islet transplantation in seven patients with type 1 diabetes mellitus using a glucocorticoid-free immunosuppressive regimen," *N Engl J Med,* vol. 343, pp. 230-8, Jul 2000.

[10]   R. M. Langer, "Islet transplantation: lessons learned since the Edmonton breakthrough," *Transplant Proc,* vol. 42, pp. 1421-4, Jun 2010.

[11]   R. M. Meloche, "Transplantation for the treatment of type 1 diabetes," *World J Gastroenterol,* vol. 13, pp. 6347-55, Dec 2007.

[12]   J. A. Giraldo, J. D. Weaver, and C. L. Stabler, "Tissue engineering approaches to enhancing clinical islet transplantation through tissue engineering strategies," *J Diabetes Sci Technol,* vol. 4, pp. 1238-47, Sep 2010.

[13]   Y. Hara, M. Fujino, K. Nakada, K. Kimura, K. Adachi, and X. K. Li, "Influence of the numbers of islets on the models of rat syngeneic-islet and allogeneic-islet transplantations," *Transplant Proc,* vol. 38, pp. 2726-8, Oct 2006.

[14]   S. Paraskevas, D. Maysinger, R. Wang, T. P. Duguid, and L. Rosenberg, "Cell loss in isolated human islets occurs by apoptosis," *Pancreas,* vol. 20, pp. 270-6, Apr 2000.

[15]   J. T. Wilson and E. L. Chaikof, "Challenges and emerging technologies in the immunoisolation of cells and tissues," *Adv Drug Deliv Rev,* vol. 60, pp. 124-45, Jan 14 2008.

[16]   S. A. Nanji and A. M. Shapiro, "Advances in pancreatic islet transplantation in humans," *Diabetes Obes Metab,* vol. 8, pp. 15-25, Jan 2006.

[17]   L. M. Weber, J. He, B. Bradley, K. Haskins, and K. S. Anseth, "PEG-based hydrogels as an in vitro encapsulation platform for testing controlled beta-cell microenvironments," *Acta Biomater,* vol. 2, pp. 1-8, Jan 2006.

[18]   H. Yagi, A. Soto-Gutierrez, B. Parekkadan, Y. Kitagawa, R. G. Tompkins, N. Kobayashi, and M. L. Yarmush, "Mesenchymal stem cells: Mechanisms of immunomodulation and homing," *Cell Transplant,* vol. 19, pp. 667-79, 2010.

[19]   R. Tasso, C. Ilengo, R. Quarto, R. Cancedda, R. R. Caspi, and G. Pennesi, "Mesenchymal stem cells induce functionally active T-regulatory lymphocytes in a paracrine fashion and ameliorate experimental autoimmune uveitis," *Invest Ophthalmol Vis Sci,* vol. 53, pp. 786-93, Feb 2012.

[20]   R. A. Boomsma and D. L. Geenen, "Mesenchymal stem cells secrete multiple cytokines that promote angiogenesis and have contrasting effects on chemotaxis and apoptosis," *PLoS One,* vol. 7, p. e35685, 2012.

[21]   R. H. Lee, M. J. Seo, R. L. Reger, J. L. Spees, A. A. Pulin, S. D. Olson, and D. J. Prockop, "Multipotent stromal cells from human marrow home to and promote repair of pancreatic islets and renal glomeruli in diabetic NOD/scid mice," *Proc Natl Acad Sci U S A,* vol. 103, pp. 17438-43, Nov 2006.

[22] L. T. Lock and E. S. Tzanakakis, "Stem/Progenitor cell sources of insulin-producing cells for the treatment of diabetes," *Tissue Eng,* vol. 13, pp. 1399-412, Jul 2007.

[23] S. Bonner-Weir, M. Taneja, G. C. Weir, K. Tatarkiewicz, K. H. Song, A. Sharma, and J. J. O'Neil, "In vitro cultivation of human islets from expanded ductal tissue," *Proc Natl Acad Sci U S A,* vol. 97, pp. 7999-8004, Jul 2000.

[24] Y. Dor, J. Brown, O. I. Martinez, and D. A. Melton, "Adult pancreatic beta-cells are formed by self-duplication rather than stem-cell differentiation," *Nature,* vol. 429, pp. 41-6, May 2004.

[25] B. E. Tuch, T. C. Hughes, and M. D. Evans, "Encapsulated pancreatic progenitors derived from human embryonic stem cells as a therapy for insulin-dependent diabetes," *Diabetes Metab Res Rev,* vol. 27, pp. 928-32, Nov 2011.

[26] J. Daoud, L. Rosenberg, and M. Tabrizian, "Pancreatic islet culture and preservation strategies: advances, challenges, and future outlook," *Cell Transplant,* vol. 19, pp. 1523-35, 2010.

[27] C. C. Lin, A. Raza, and H. Shih, "PEG hydrogels formed by thiol-ene photo-click chemistry and their effect on the formation and recovery of insulin-secreting cell spheroids," *Biomaterials,* vol. 32, pp. 9685-95, Dec 2011.

[28] Y. E. Souza, E. Chaib, P. G. Lacerda, A. Crescenzi, A. Bernal-Filho, and L. A. D'Albuquerque, "Islet transplantation in rodents. Do encapsulated islets really work?," *Arq Gastroenterol,* vol. 48, pp. 146-52, Apr-Jun 2011.

[29] C. C. Lin, A. T. Metters, and K. S. Anseth, "Functional PEG-peptide hydrogels to modulate local inflammation induced by the pro-inflammatory cytokine TNFalpha," *Biomaterials,* vol. 30, pp. 4907-14, Oct 2009.

[30] C. C. Lin, P. D. Boyer, A. A. Aimetti, and K. S. Anseth, "Regulating MCP-1 diffusion in affinity hydrogels for enhancing immuno-isolation," *J Control Release,* vol. 142, pp. 384-91, Mar 2010.

[31] P. S. Hume, C. N. Bowman, and K. S. Anseth, "Functionalized PEG hydrogels through reactive dip-coating for the formation of immunoactive barriers," *Biomaterials,* vol. 32, pp. 6204-12, Sep 2011.

[32] L. M. Weber, K. N. Hayda, and K. S. Anseth, "Cell-matrix interactions improve beta-cell survival and insulin secretion in three-dimensional culture," *Tissue Eng Part A,* vol. 14, pp. 1959-68, Dec 2008.

[33] S. Kizilel, M. Garfinkel, and E. Opara, "The bioartificial pancreas: progress and challenges," *Diabetes Technol Ther,* vol. 7, pp. 968-85, Dec 2005.

[34] E. Pedraza, M. M. Coronel, C. A. Fraker, C. Ricordi, and C. L. Stabler, "Preventing hypoxia-induced cell death in beta cells and islets via hydrolytically activated, oxygen-generating biomaterials," *Proc Natl Acad Sci U S A,* vol. 109, pp. 4245-50, Mar 2012.

[35] C. C. Lin and K. S. Anseth, "Glucagon-like peptide-1 functionalized PEG hydrogels promote survival and function of encapsulated pancreatic beta-cells," *Biomacromolecules,* vol. 10, pp. 2460-7, Sep 2009.

[36] K. Kimoto, K. Suzuki, T. Kizaki, Y. Hitomi, H. Ishida, H. Katsuta, E. Itoh, T. Ookawara, K. Honke, and H. Ohno, "Gliclazide protects pancreatic beta-cells from damage by hydrogen peroxide," *Biochem Biophys Res Commun,* vol. 303, pp. 112-9, Mar 2003.

[37] N. Hou, S. Torii, N. Saito, M. Hosaka, and T. Takeuchi, "Reactive oxygen species-mediated pancreatic beta-cell death is regulated by interactions between stress-activated protein kinases, p38 and c-Jun N-terminal kinase, and mitogen-activated protein kinase phosphatases," *Endocrinology,* vol. 149, pp. 1654-65, Apr 2008.

[38] M. W. Tibbitt and K. S. Anseth, "Hydrogels as extracellular matrix mimics for 3D cell culture," *Biotechnol Bioeng,* vol. 103, pp. 655-63, Jul 2009.

[39] C. C. Lin and K. S. Anseth, "PEG hydrogels for the controlled release of biomolecules in regenerative medicine," *Pharm Res,* vol. 26, pp. 631-43, Mar 2009.

[40] C. C. Lin and A. T. Metters, "Hydrogels in controlled release formulations: network design and mathematical modeling," *Adv Drug Deliv Rev,* vol. 58, pp. 1379-408, Nov 2006.

[41] A. S. Hoffman, "Hydrogels for biomedical applications," *Adv Drug Deliv Rev,* vol. 54, pp. 3-12, Jan 2002.

[42] J. Zhu, "Bioactive modification of poly(ethylene glycol) hydrogels for tissue engineering," *Biomaterials,* vol. 31, pp. 4639-56, Jun 2010.

[43] C. C. Lin and K. S. Anseth, "Controlling Affinity Binding with Peptide-Functionalized Poly(ethylene glycol) Hydrogels," *Adv Funct Mater,* vol. 19, p. 2325, Jul 2009.

[44] A. Khademhosseini and R. Langer, "Microengineered hydrogels for tissue engineering," *Biomaterials,* vol. 28, pp. 5087-92, Dec 2007.

[45] J. L. Ifkovits and J. A. Burdick, "Review: photopolymerizable and degradable biomaterials for tissue engineering applications," *Tissue Eng,* vol. 13, pp. 2369-85, Oct 2007.

[46] J. A. Burdick and K. S. Anseth, "Photoencapsulation of osteoblasts in injectable RGD-modified PEG hydrogels for bone tissue engineering," *Biomaterials,* vol. 23, pp. 4315-23, Nov 2002.

[47] E. Jabbari, "Bioconjugation of hydrogels for tissue engineering," *Curr Opin Biotechnol,* vol. 22, pp. 655-60, Oct 2011.

[48] B. V. Slaughter, S. S. Khurshid, O. Z. Fisher, A. Khademhosseini, and N. A. Peppas, "Hydrogels in regenerative medicine," *Adv Mater,* vol. 21, pp. 3307-29, Sep 2009.

[49] L. M. Weber, K. N. Hayda, K. Haskins, and K. S. Anseth, "The effects of cell-matrix interactions on encapsulated beta-cell function within hydrogels functionalized with matrix-derived adhesive peptides," *Biomaterials,* vol. 28, pp. 3004-11, Jul 2007.

[50] J. Su, B. H. Hu, W. L. Lowe, Jr., D. B. Kaufman, and P. B. Messersmith, "Anti-inflammatory peptide-functionalized hydrogels for insulin-secreting cell encapsulation," *Biomaterials,* vol. 31, pp. 308-14, Jan 2010.

[51] D. S. Benoit, A. R. Durney, and K. S. Anseth, "The effect of heparin-functionalized PEG hydrogels on three-dimensional human mesenchymal stem cell osteogenic differentiation," *Biomaterials,* vol. 28, pp. 66-77, Jan 2007.

[52] N. S. Hwang, S. Varghese, H. Li, and J. Elisseeff, "Regulation of osteogenic and chondrogenic differentiation of mesenchymal stem cells in PEG-ECM hydrogels," *Cell Tissue Res,* vol. 344, pp. 499-509, Jun 2011.

[53] A. A. Aimetti, M. W. Tibbitt, and K. S. Anseth, "Human neutrophil elastase responsive delivery from poly(ethylene glycol) hydrogels," *Biomacromolecules,* vol. 10, pp. 1484-9, Jun 2009.

[54] S. P. Zustiak, R. Durbal, and J. B. Leach, "Influence of cell-adhesive peptide ligands on poly(ethylene glycol) hydrogel physical, mechanical and transport properties," *Acta Biomater,* vol. 6, pp. 3404-14, Sep 2010.

[55] C. C. Lin and K. S. Anseth, "Cell-cell communication mimicry with poly(ethylene glycol) hydrogels for enhancing beta-cell function," *Proc Natl Acad Sci U S A,* vol. 108, pp. 6380-5, Apr 2011.

[56] H. Hui, A. Nourparvar, X. Zhao, and R. Perfetti, "Glucagon-like peptide-1 inhibits apoptosis of insulin-secreting cells via a cyclic 5'-adenosine monophosphate-dependent protein kinase A- and a phosphatidylinositol 3-kinase-dependent pathway," *Endocrinology,* vol. 144, pp. 1444-55, Apr 2003.

[57] L. M. Weber, C. G. Lopez, and K. S. Anseth, "Effects of PEG hydrogel crosslinking density on protein diffusion and encapsulated islet survival and function," *J Biomed Mater Res A,* vol. 90, pp. 720-9, Sep 2009.

[58] C. C. Lin and A. T. Metters, "Enhanced protein delivery from photopolymerized hydrogels using a pseudospecific metal chelating ligand," *Pharm Res,* vol. 23, pp. 614-22, Mar 2006.

[59] J. D. McCall and K. S. Anseth, "Thiol-ene photopolymerizations provide a facile method to encapsulate proteins and maintain their bioactivity," *Biomacromolecules,* vol. 13, pp. 2410-7, Aug 2012.

[60] C. W. Hsu, R. M. Olabisi, E. A. Olmsted-Davis, A. R. Davis, and J. L. West, "Cathepsin K-sensitive poly(ethylene glycol) hydrogels for degradation in response to bone resorption," *J Biomed Mater Res A,* vol. 98, pp. 53-62, Jul 2011.

[61] J. E. Leslie-Barbick, J. J. Moon, and J. L. West, "Covalently-immobilized vascular endothelial growth factor promotes endothelial cell tubulogenesis in poly(ethylene glycol) diacrylate hydrogels," *J Biomater Sci Polym Ed,* vol. 20, pp. 1763-79, 2009.

[62] J. J. Moon, M. S. Hahn, I. Kim, B. A. Nsiah, and J. L. West, "Micropatterning of poly(ethylene glycol) diacrylate hydrogels with biomolecules to regulate and guide endothelial morphogenesis," *Tissue Eng Part A,* vol. 15, pp. 579-85, Mar 2009.

[63] B. D. Fairbanks, M. P. Schwartz, A. E. Halevi, C. R. Nuttelman, C. N. Bowman, and K. S. Anseth, "A Versatile Synthetic Extracellular Matrix Mimic via Thiol-Norbornene Photopolymerization," *Advanced Materials,* vol. 21, pp. 5005-10, Dec 2009.

[64] J. A. Benton, B. D. Fairbanks, and K. S. Anseth, "Characterization of valvular interstitial cell function in three dimensional matrix metalloproteinase degradable PEG hydrogels," *Biomaterials,* vol. 30, pp. 6593-603, Dec 2009.

[65]   A. A. Aimetti, A. J. Machen, and K. S. Anseth, "Poly(ethylene glycol) hydrogels formed by thiol-ene photopolymerization for enzyme-responsive protein delivery," *Biomaterials,* vol. 30, pp. 6048-54, Oct 2009.

[66]   P. D. Mariner, J. M. Wudel, D. E. Miller, E. E. Genova, S. O. Streubel, and K. S. Anseth, "Synthetic hydrogel scaffold is an effective vehicle for delivery of INFUSE (rhBMP2) to critical-sized calvaria bone defects in rats," *J Orthop Res,* vol. 31, pp. 401-6, Mar 2013.

[67]   C. E. Hoyle and C. N. Bowman, "Thiol-ene click chemistry," *Angew Chem Int Ed Engl,* vol. 49, pp. 1540-73, Feb 2010.

[68]   C. E. Hoyle, A. B. Lowe, and C. N. Bowman, "Thiol-click chemistry: a multifaceted toolbox for small molecule and polymer synthesis," *Chem Soc Rev,* vol. 39, pp. 1355-87, Apr 2010.

[69]   A. Raza and C.-C. Lin, "Generation and Recovery of β-cell Spheroids From Step-growth PEG-peptide Hydrogels," *J Vis Exp,* p. e50081, 2012.

[70]   H. Shih and C. C. Lin, "Cross-linking and degradation of step-growth hydrogels formed by thiol-ene photoclick chemistry," *Biomacromolecules,* vol. 13, pp. 2003-12, Jul 2012.

[71]   M. Lieber, J. Mazzetta, W. Nelson-Rees, M. Kaplan, and G. Todaro, "Establishment of a continuous tumor-cell line (panc-1) from a human carcinoma of the exocrine pancreas," *Int J Cancer,* vol. 15, pp. 741-7, May 1975.

[72]   M. E. Madden and M. P. Sarras, Jr., "Morphological and biochemical characterization of a human pancreatic ductal cell line (PANC-1)," *Pancreas,* vol. 3, pp. 512-28, 1988.

[73]   S. Githens, "The pancreatic duct cell: proliferative capabilities, specific characteristics, metaplasia, isolation, and culture," *J Pediatr Gastroenterol Nutr,* vol. 7, pp. 486-506, Jul-Aug 1988.

[74]   K. Zhang, X. Jiao, X. Liu, B. Zhang, J. Wang, Q. Wang, Y. Tao, and D. Zhang, "Knockdown of snail sensitizes pancreatic cancer cells to chemotherapeutic agents and irradiation," *Int J Mol Sci,* vol. 11, pp. 4891-2, 2010.

[75] K. B. Harikumar, A. B. Kunnumakkara, N. Ochi, Z. Tong, A. Deorukhkar, B. Sung, L. Kelland, S. Jamieson, R. Sutherland, T. Raynham, M. Charles, A. Bagherzadeh, C. Foxton, A. Boakes, M. Farooq, D. Maru, P. Diagaradjane, Y. Matsuo, J. Sinnett-Smith, J. Gelovani, S. Krishnan, B. B. Aggarwal, E. Rozengurt, C. R. Ireson, and S. Guha, "A novel small-molecule inhibitor of protein kinase D blocks pancreatic cancer growth in vitro and in vivo," *Mol Cancer Ther,* vol. 9, pp. 1136-46, May 2010.

[76] Y. Matsuda, Z. Naito, K. Kawahara, N. Nakazawa, M. Korc, and T. Ishiwata, "Nestin is a novel target for suppressing pancreatic cancer cell migration, invasion and metastasis," *Cancer Biol Ther,* vol. 11, pp. 512-23, Mar 2011.

[77] J. H. Zhang, F. J. Lai, H. Chen, J. Luo, R. Y. Zhang, H. Q. Bu, Z. H. Wang, H. H. Lin, and S. Z. Lin, "Involvement of the phosphoinositide 3-kinase/Akt pathway in apoptosis induced by capsaicin in the human pancreatic cancer cell line PANC-1," *Oncol Lett,* vol. 5, pp. 43-48, Jan 2013.

[78] L. Han, H. W. Zhang, W. P. Zhou, G. M. Chen, and K. J. Guo, "The effects of genistein on transforming growth factor-beta1-induced invasion and metastasis in human pancreatic cancer cell line Panc-1 in vitro," *Chin Med J (Engl),* vol. 125, pp. 2032-40, Jun 2012.

[79] M. G. Binker, A. A. Binker-Cosen, D. Richards, B. Oliver, and L. I. Cosen-Binker, "EGF promotes invasion by PANC-1 cells through Rac1/ROS-dependent secretion and activation of MMP-2," *Biochem Biophys Res Commun,* vol. 379, pp. 445-50, Feb 2009.

[80] X. Y. Zhu, N. Liu, W. Liu, S. W. Song, and K. J. Guo, "Silencing of the integrin-linked kinase gene suppresses the proliferation, migration and invasion of pancreatic cancer cells (Panc-1)," *Genet Mol Biol,* vol. 35, pp. 538-44, Apr 2012.

[81] H. Hui, C. Wright, and R. Perfetti, "Glucagon-like peptide 1 induces differentiation of islet duodenal homeobox-1-positive pancreatic ductal cells into insulin-secreting cells," *Diabetes,* vol. 50, pp. 785-96, Apr 2001.

[82] A. A. Hardikar, B. Marcus-Samuels, E. Geras-Raaka, B. M. Raaka, and M. C. Gershengorn, "Human pancreatic precursor cells secrete FGF2 to stimulate clustering into hormone-expressing islet-like cell aggregates," *Proc Natl Acad Sci U S A,* vol. 100, pp. 7117-22, Jun 2003.

[83] Y. Wu, J. Li, S. Saleem, S. P. Yee, A. A. Hardikar, and R. Wang, "c-Kit and stem cell factor regulate PANC-1 cell differentiation into insulin- and glucagon-producing cells," *Lab Invest,* vol. 90, pp. 1373-84, Sep 2010.

[84]   J. Li, Y. Wang, X. Yu, H. Chen, Y. Wu, X. Han, X. Guo, C. Zhang, Q. Chen, J. Chen, and T. Yang, "Islet neogenesis-associated protein-related pentadecapeptide enhances the differentiation of islet-like clusters from human pancreatic duct cells," *Peptides,* vol. 30, pp. 2242-9, Dec 2009.

[85]   M. A. Shields, S. Dangi-Garimella, S. B. Krantz, D. J. Bentrem, and H. G. Munshi, "Pancreatic cancer cells respond to type I collagen by inducing snail expression to promote membrane type 1 matrix metalloproteinase-dependent collagen invasion," *J Biol Chem,* vol. 286, pp. 10495-504, Mar 2011.

[86]   Y. Kitaura, N. Chikazawa, T. Tasaka, K. Nakano, M. Tanaka, H. Onishi, and M. Katano, "Transforming growth factor beta1 contributes to the invasiveness of pancreatic ductal adenocarcinoma cells through the regulation of CD24 expression," *Pancreas,* vol. 40, pp. 1034-42, Oct 2011.

[87]   M. A. Shields, S. Dangi-Garimella, A. J. Redig, and H. G. Munshi, "Biochemical role of the collagen-rich tumour microenvironment in pancreatic cancer progression," *Biochem J,* vol. 441, pp. 541-52, Jan 2012.

[88]   B. D. Fairbanks, M. P. Schwartz, C. N. Bowman, and K. S. Anseth, "Photoinitiated polymerization of PEG-diacrylate with lithium phenyl-2,4,6-trimethylbenzoylphosphinate: polymerization rate and cytocompatibility," *Biomaterials,* vol. 30, pp. 6702-7, Dec 2009.

[89]   S. Netzel-Arnett, Q. X. Sang, W. G. Moore, M. Navre, H. Birkedal-Hansen, and H. E. Van Wart, "Comparative sequence specificities of human 72- and 92-kDa gelatinases (type IV collagenases) and PUMP (matrilysin)," *Biochemistry,* vol. 32, pp. 6427-32, Jun 1993.

[90]   H. Nagase and G. B. Fields, "Human matrix metalloproteinase specificity studies using collagen sequence-based synthetic peptides," *Biopolymers,* vol. 40, pp. 399-416, 1996.

[91]   M. P. Lutolf, J. L. Lauer-Fields, H. G. Schmoekel, A. T. Metters, F. E. Weber, G. B. Fields, and J. A. Hubbell, "Synthetic matrix metalloproteinase-sensitive hydrogels for the conduction of tissue regeneration: engineering cell-invasion characteristics," *Proc Natl Acad Sci U S A,* vol. 100, pp. 5413-8, Apr 2003.

[92]   S. B. Anderson, C. C. Lin, D. V. Kuntzler, and K. S. Anseth, "The performance of human mesenchymal stem cells encapsulated in cell-degradable polymer-peptide hydrogels," *Biomaterials,* vol. 32, pp. 3564-74, May 2011.

[93]   A. Shikanov, R. M. Smith, M. Xu, T. K. Woodruff, and L. D. Shea, "Hydrogel network design using multifunctional macromers to coordinate tissue maturation in ovarian follicle culture," *Biomaterials,* vol. 32, pp. 2524-31, Apr 2011.

[94]   C. S. Bahney, T. J. Lujan, C. W. Hsu, M. Bottlang, J. L. West, and B. Johnstone, "Visible light photoinitiation of mesenchymal stem cell-laden bioresponsive hydrogels," *Eur Cell Mater,* vol. 22, pp. 43-55; discussion 55, 2011.

[95]   X. Yang, S. K. Sarvestani, S. Moeinzadeh, X. He, and E. Jabbari, "Three-Dimensional-Engineered Matrix to Study Cancer Stem Cells and Tumorsphere Formation: Effect of Matrix Modulus," *Tissue Eng Part A,* Nov 2012.

[96]   Z. G. Chang, J. M. Wei, C. F. Qin, K. Hao, X. D. Tian, K. Xie, X. H. Xie, and Y. M. Yang, "Suppression of the epidermal growth factor receptor inhibits epithelial-mesenchymal transition in human pancreatic cancer PANC-1 cells," *Dig Dis Sci,* vol. 57, pp. 1181-9, May 2012.

[97]   C. S. Bahney, C. W. Hsu, J. U. Yoo, J. L. West, and B. Johnstone, "A bioresponsive hydrogel tuned to chondrogenesis of human mesenchymal stem cells," *FASEB J,* vol. 25, pp. 1486-96, May 2011.

[98]   J. D. McCall, J. E. Luoma, and K. S. Anseth, "Covalently tethered transforming growth factor beta in PEG hydrogels promotes chondrogenic differentiation of encapsulated human mesenchymal stem cells," *Drug Deliv Transl Res,* vol. 2, pp. 305-312, Oct 2012.

[99]   L. Jongpaiboonkit, W. J. King, and W. L. Murphy, "Screening for 3D environments that support human mesenchymal stem cell viability using hydrogel arrays," *Tissue Eng Part A,* vol. 15, pp. 343-53, Feb 2009.

[100] W. J. King, L. Jongpaiboonkit, and W. L. Murphy, "Influence of FGF2 and PEG hydrogel matrix properties on hMSC viability and spreading," *J Biomed Mater Res A,* vol. 93, pp. 1110-23, Jun 2010.

[101] G. A. Hudalla, T. S. Eng, and W. L. Murphy, "An approach to modulate degradation and mesenchymal stem cell behavior in poly(ethylene glycol) networks," *Biomacromolecules,* vol. 9, pp. 842-9, Mar 2008.

[102] L. Gao, R. McBeath, and C. S. Chen, "Stem cell shape regulates a chondrogenic versus myogenic fate through Rac1 and N-cadherin," *Stem Cells,* vol. 28, pp. 564-72, Mar 2010.

[103] L. F. Sempere, J. R. Gunn, and M. Korc, "A novel 3-dimensional culture system uncovers growth stimulatory actions by TGFbeta in pancreatic cancer cells," *Cancer Biol Ther,* vol. 12, pp. 198-207, Aug 2011.

[104] Y. Matsuda, T. Ishiwata, Y. Kawamoto, K. Kawahara, W. X. Peng, T. Yamamoto, and Z. Naito, "Morphological and cytoskeletal changes of pancreatic cancer cells in three-dimensional spheroidal culture," *Med Mol Morphol,* vol. 43, pp. 211-7, Dec 2010.

[105] S. Zhu, Y. Zhou, L. Wang, J. Zhang, H. Wu, J. Xiong, Y. Tian, and C. Wang, "Transcriptional upregulation of MT2-MMP in response to hypoxia is promoted by HIF-1alpha in cancer cells," *Mol Carcinog,* vol. 50, pp. 770-80, Oct 2011.

[106] A. Miyoshi, Y. Kitajima, T. Ide, K. Ohtaka, H. Nagasawa, Y. Uto, H. Hori, and K. Miyazaki, "Hypoxia accelerates cancer invasion of hepatoma cells by upregulating MMP expression in an HIF-1alpha-independent manner," *Int J Oncol,* vol. 29, pp. 1533-9, Dec 2006.

[107] B. A. Katchman, K. Antwi, G. Hostetter, M. J. Demeure, A. Watanabe, G. A. Decker, L. J. Miller, D. D. Von Hoff, and D. F. Lake, "Quiescin sulfhydryl oxidase 1 promotes invasion of pancreatic tumor cells mediated by matrix metalloproteinases," *Mol Cancer Res,* vol. 9, pp. 1621-31, Dec 2011.

[108] V. Bister, T. Skoog, S. Virolainen, T. Kiviluoto, P. Puolakkainen, and U. Saarialho-Kere, "Increased expression of matrix metalloproteinases-21 and -26 and TIMP-4 in pancreatic adenocarcinoma," *Mod Pathol,* vol. 20, pp. 1128-40, Nov 2007.

[109] H. Yamamoto, F. Itoh, S. Iku, Y. Adachi, H. Fukushima, S. Sasaki, M. Mukaiya, K. Hirata, and K. Imai, "Expression of matrix metalloproteinases and tissue inhibitors of metalloproteinases in human pancreatic adenocarcinomas: clinicopathologic and prognostic significance of matrilysin expression," *J Clin Oncol,* vol. 19, pp. 1118-27, Feb 2001.

[110] M. Lukaszewicz, B. Mroczko, and M. Szmitkowski, "[The role of metalloproteinases and their inhibitors in pancreatic cancer]," *Postepy Hig Med Dosw (Online),* vol. 62, pp. 141-7, 2008.

[111] A. M. Jamal, M. Lipsett, A. Hazrati, S. Paraskevas, D. Agapitos, D. Maysinger, and L. Rosenberg, "Signals for death and differentiation: a two-step mechanism for in vitro transformation of adult islets of Langerhans to duct epithelial structures," *Cell Death Differ,* vol. 10, pp. 987-96, Sep 2003.

[112] I. M. Chung, N. O. Enemchukwu, S. D. Khaja, N. Murthy, A. Mantalaris, and A. J. Garcia, "Bioadhesive hydrogel microenvironments to modulate epithelial morphogenesis," *Biomaterials,* vol. 29, pp. 2637-45, Jun 2008.

[113] S. Hamada, K. Satoh, A. Masamune, and T. Shimosegawa, "Regulators of epithelial mesenchymal transition in pancreatic cancer," *Front Physiol,* vol. 3, p. 254, 2012.

[114] B. Dave, V. Mittal, N. M. Tan, and J. C. Chang, "Epithelial-mesenchymal transition, cancer stem cells and treatment resistance," *Breast Cancer Res,* vol. 14, p. 202, 2012.

[115] A. M. Kloxin, C. J. Kloxin, C. N. Bowman, and K. S. Anseth, "Mechanical properties of cellularly responsive hydrogels and their experimental determination," *Advanced Materials,* vol. 22, pp. 3484-94, Aug 2010.

[116] T. P. Appelman, J. Mizrahi, J. H. Elisseeff, and D. Seliktar, "The differential effect of scaffold composition and architecture on chondrocyte response to mechanical stimulation," *Biomaterials,* vol. 30, pp. 518-25, Feb 2009.

[117] S. J. Bryant, K. S. Anseth, D. A. Lee, and D. L. Bader, "Crosslinking density influences the morphology of chondrocytes photoencapsulated in PEG hydrogels during the application of compressive strain," *J Orthop Res,* vol. 22, pp. 1143-9, Sep 2004.

[118] J. L. Leight, M. A. Wozniak, S. Chen, M. L. Lynch, and C. S. Chen, "Matrix rigidity regulates a switch between TGF-beta1-induced apoptosis and epithelial-mesenchymal transition," *Mol Biol Cell,* vol. 23, pp. 781-91, Mar 2012.

[119] J. S. Miller, C. J. Shen, W. R. Legant, J. D. Baranski, B. L. Blakely, and C. S. Chen, "Bioactive hydrogels made from step-growth derived PEG-peptide macromers," *Biomaterials,* vol. 31, pp. 3736-43, May 2010.

[120] E. A. Phelps, N. O. Enemchukwu, V. F. Fiore, J. C. Sy, N. Murthy, T. A. Sulchek, T. H. Barker, and A. J. Garcia, "Maleimide cross-linked bioactive PEG hydrogel exhibits improved reaction kinetics and cross-linking for cell encapsulation and in situ delivery," *Adv Mater,* vol. 24, pp. 64-70, 2, Jan 2012.

[121] M. S. Weiss, B. P. Bernabe, A. Shikanov, D. A. Bluver, M. D. Mui, S. Shin, L. J. Broadbelt, and L. D. Shea, "The impact of adhesion peptides within hydrogels on the phenotype and signaling of normal and cancerous mammary epithelial cells," *Biomaterials,* vol. 33, pp. 3548-59, May 2012.